CZECH UNIVERSITY OF LIFE SCIENCES PRAGUE

Department of Water Resources and Environmental Modeling

Faculty of Environmental Sciences

DIPLOMA THESIS ASSIGNMENT

Kingsley Onyeka Ezeji

Environmental Modelling

Thesis title

Reactive transport modeling in porous media

Objectives of thesis

Evaluation of sorption of heavy metals on biochar media, laboratory experiments and mathematical model evaluation

Methodology

- literature retrieval
- laboratory sorption experiments
- data postprocessing
- selection of mathematical model for kinetic model
- parameter fitting

The proposed extent of the thesis
60 pages

Keywords
kinetic sorption, equilibrium sorption, biochar, heavy metals, decay law

---

Recommended information sources
FETTER, C W. *Applied hydrogeology.* Upper Saddle River, NJ: Prentice Hall, 2001. ISBN 9780130882394.

Expected date of thesis defence
2015/06 (červen)

The Diploma Thesis Supervisor
Ing. Michal Kuráž, Ph.D.

Advisor of thesis
Mgr. Lukas Trakal, PhD.

Electronic approval: 20. 4. 2015

prof. Ing. Pavel Pech, CSc.

Head of department

Electronic approval: 21. 4. 2015

prof. Ing. Petr Sklenička, CSc.

Dean

Prague on 22. 04. 2015

Czech University of Life Sciences

Masters Thesis

Reactive Transport Modelling in Porous Media

Author:
Kingsley Onyeka EZEJI

Supervisor:
Dr. Mikal Kuraz

A thesis submitted in fulfilment of the requirements
for the degree of Master of Science in Environmental Modelling

in the

Faculty of Environmental Sciences
Department of Water Resources and Environmental Modelling

April 22, 2015

Declaration of Authorship

I, Kingsley Onyeka EZEJI, hereby declares that this thesis with the title 'Reactive Transport Modelling in Porous Media' and the results presented in it are of my own effort. I confirm that:

- The work presented was done mainly while enrolled for a masters degree program at this University.
- Sections of this thesis, Which has been previously submitted for a degree or other qualification at this University or other university, this has been stated clearly.
- Where the published work of authors were consulted, it is always clearly attributed.
- In sections Where the work of others were quoted, the source is always indicated. in absence of such quotations, this thesis is entirely my own work.
- All the main sources of help have been duly acknowledged.
- In sections of the thesis, where work done is in collaboration with others, I have clearly stated exactly what I have contributed myself and what was done by others.

Signed: _____

Date: _____

"Imagination is more important than knowledge. Knowledge is limited. Imagination encircles the world."

Albert Einstein

CZECH UNIVERSITY OF LIFE SCIENCES

Abstract

Faculty of Environmental sciences
Department of Water Resources and Environmental Modelling

Master of Science in Environmental Modelling

Reactive Transport Modelling in Porous Media

by Kingsley Onyeka EZEJI

The main aim of this thesis was to evaluate the mechanisms and characteristics of $Pb(II)$ sorption by biochar which was produced from grape stalks ($GSBC$) at pH of 5.Different initial $Pb(II)$ concentrations of $1mM$, $0.2mM$ and $0.1mM$, were examined. The Pb sorption isotherms and kinetics were investigated.

The biochar was quite effective in $Pb(II)$ sorption with a maximum sorption capacity which showed an increase from 10 to $15mg.g^{-1}$ as initial $Pb(II)$ concentration increased from $0.1mM$ to $0.2mM$. Increased alkaline earth metal cations concentration indicated that ion exchange was also responsible for $Pb(II)$ sorption. Initial $Pb(II)$ concentration significantly affected biochar properties and played an important role in Pb sorption mechanisms and capacity by biochar.

The kinetic data from the sorption experiment were analysed with the use of batch kinetics and analytically, using the pseudo-first and-second order kinetic models and and intraparticle diffusion equation. The equilibrium sorption capacities ,rate constants, kinetic parameters and the associated correlation coefficients for the applied kinetic model were determined and discussed.Sorption by ion exchange was studied by comparing the total amount of sorped $Pb(II)$ to the total amount of initially sorbed calcium, potassium and magnesium cations released.

The results showed the sorption kinetics followed both the pseudo-first and-second order kinetic model, with relatively high amounts of potassium cations released into the solution, suggesting that the mechanisms of sorption presumably follows a physio-sorption, chemi-sorption and ion- exchange process

Keywords: Kinetic sorption, equilibrium sorption, biochar, heavy metals, decay law...

Acknowledgements

I wish to acknowledge the overwhelming support by my thesis supervisor, Dr. Mikal Kuraz and academic consultant for their immense guidance and practical training, unwavering support, and warm friendship throughout the period of my research. Their words of encouragement helped to boost my faith in myself as a researcher; the fact that the accomplished work may become a significant contribution to the development of environmentally efficient technology. In the fueling of my drive in continuation of the pursuit of my scientific career, I am very grateful to both of them.

My warm gratitude goes to Silva Cihalova, who was patient and generous a enough in assisting me run the ICP-MS, despite my excess of samples. She has been instrumental in seeing to the success of not just my own thesis experiment, but also for those of other thesis students who worked in the Geochemistry laboratory.

I send special thanks to all members of the department of the Environmental science faculty who have made the last two academic years an interesting interdisciplinary and cross-cultural experience.

Acknowledgments also goes to my parents and siblings, for which without their support and unconditional love, I would not have made it this far. Finally, I wish to thank my wonderful wife, Alena, who has had to tolerate my long hours of work and has been a steadfast partner in everything. I thank you very much for being my all-around emotional and technical support through the last two years. I could not have made it to the end without you...

Contents

List of Figures

List of Tables

Abbreviations

REV	**R**epresentative **V**olume **E**lement
ADE	**A**dvection **D**ispersion **E**quation
FDM	**F**inite **D**ifference **M**ethod
FEM	**F**inite **E**lement **M**ethod
PDE	**P**artial **D**ifferential **E**quation
ICP-OES	**I**nductively **C**oupled **P**lasma **O**ptical **E**mission **S**pectroscopy
GSBC	**G**rape **S**talks **B**io **C**har
CEC	**C**ation **E**xchange **C**apacity

Physical Constants

Acceleration due to gravity $g = 9.897\text{ms}^{-2}$ (exact)

Symbols

ϕ	effective porosity	-
τ	tortuosity	-
αi	dispersivity tensor	
ϕ_t	total porosity	-
∇H	hydraulic gradient	L/L
λ	decay constant	-
Ω	domain of PDE problem	-
$\partial\Omega$	boundary segment of the Ω domain	-
$\vec{J}$	mass flux of solute per unit area per unit time	M/L^2/T
$\vec{J}_{adv}$	advective flux	M/L^2/T
$\vec{J}_{dis}$	dispersive flux	M/L^2/T
$\vec{J}_{dif}$	diffusive flux	M/L^2/T
D_*	diffusion coefficient	L^2/T
R	retardation coefficient	M/L^3
D_m	molecular diffusion coefficient	L^2/T
c	solute concentration	M/L^3
∇c	concentration gradient	M/L^3/L
c_0	initial liquid phase lead concentration	M/L^3
K_1	rate constant for pseudo-second order sorption	T^{-1}
K_2	rate constant for pseudo-second order sorption	M(biochar)/M(Pb)/T
K_{id}	intra-particle diffusion rate coefficient	M/M/T
K_L	Langmuir equilibrium constant	L^3/M
K_F	Freundlich equilibrium constant	M/ML^3/M
D^*	dispersion coefficient	L^2/T
g	gravitational acceleration	L/T^2

ρ	mass density of fluid	$\mathrm{M/L^3}$
ρ_b	bulk density of fluid	$\mathrm{M/L^3}$
$\vec{v}_*$	average linear velocity	L/T
$\vec{q}_*$	darcy velocity or volume flux	L/T
θ	moisture content	
$\mathbf{K}$	hydraulic conductivity tensor	L/T
K_s	unsaturated hydraulic conductivity	L/T
K	saturated hydraulic conductivity	L/T
H	hydraulic head	L
h	Capillary pressure head	L
z	geodetic head	L
t	sorption contact time,	T
S_s	specific storage	L^{-1}
G	source/sink term	L^3/T
dA	elemental cross sectional area	L^2
V	volume of solution	L^3
r^2	Coefficient of determination	$(-)$
P	number of polar sites on the biochar surface	$(-)$
q_t	amount of metal ion sorbed at time t	$M(Pb).M^{-1}(biochar)$
q_e	amount of metal ion sorbed at time equilibrium	$M(Pb).M^{-1}(biochar)$
M^{2+}	metal cation	$(-)$
m	sorbent mass	M
SS_{tot}	The total sum of squares	$(-)$
SS_{res}	The residual sum of squares	$(-)$
n	reciprocal of Freundlich exponent	$(-)$

To my one. . .

Chapter 1

Introduction

1.1 Objectives and Background of the study

In recent years there has been increasing attention directed towards the modeling of transport processes occuring in the unsaturated or the vadose zone. This unsaturated zone is typically positioned between the groundwater level and the surface of the soil and constitutes a major element in the hydrological cycle. most chemical substances are transported by infiltrating the water through the unsaturated zone and could at the same time contaminate the groundwater. The nature of such chemical subtances, herewith referred to as contaminants may be very different (fertilizers, pathogenic microorganisms, pesticides, radio-nuclides, and heavy metals) possibly originating from various sources such as waste disposals, accidental oil spills industrial and agricultural activity. Therefore, it becomes crucial to be able to adequately predict the fate of contaminants for the protection of groundwater resources.

The main objectives of this thesis are to evaluate heavy metal sorption on porous media and to determine and optimize parameters to describe the sorption behavior.

Inorder to accomplish these objectives, laboratory sorption experiments is carried out followed by selection of a mathematical model for kinetic modeling of the sorption process. The heavy metal used throughout this thesis is Pb and a waste agricultural biomass known as biochar has been used as the porous media.

Contamination by Pb in the environment has been an issue of great concern due to its high level toxicity to living organism even in relatively low concentrations. To adequately setup measures in view of protection of public health, the World Health Organization and the European Community Directive of 98/83 had to set the allowable level of Pb at 10 $\mu g \cdot l^{-1}$ in drinking water as effective from December 2013 [Sublet *et al.* , 2003].Therefore, it became necessary to develop more effective and economical methods so as to remove

Pb from contaminated soil or groundwater systems.
So far, a few methods have already been developed to address the stringent environmental regulations necessitating the removal of heavy metals from soil or groundwater. conventional water treatment technologies, such as packed-bed filtration, reverse osmosis, precipitation, electro-coagulation and ion exchange have been found to be quite effective in reducing the concentrations of heavy metal.But, most of these removal technologies, however, are usually associated with a high operation cost and/or associated sludge disposal problems.

These accrued disadvantages have increased the need to develop other alternative and low-cost water treatment procedures for heavy metal contaminants.Sorbents such as biochar have therefore been suggested to be a potential candidate to satisfy the need in the removal of toxic metals from groundwater or soil [Trakal *et al.* , 2014].

Inorder to adequately predict the transport and fate of contaminants (Pb for example) in porous media, most researchers commonly rely on the maximum adsorption levels and distribution coefficients which are obtained from laboratory experiments where its assumed the reaction attains equilibrium. However, most reactions occuring in the environment are rarely at equilibrium, rather are in usually in a continuously changing state due to the dynamic processes taking place (Sparks [2013]; Wang [2010]). One other factor that causes discrepancies in predicting contaminant behavior is the neglect of subsequent desorption processes, which tends to be a crucial process controlling bioavailability of heavy metals in the environment. Thus, it is highly critical that time-dependent metal sorption and subsequent desorption reaction mechanisms on soil or amended soil be well understood, so as to be able to make better modelling and predictions about mobility of the contaminants and improve remediation strategies.

1.2 Scope and Limitations

The work done in this thesis is aimed at the analysis of sorption of heavy metals on biochar media using the kinetic approach. The work has three main approach. First is the retrieval of related information from existing literature .The second approach is the execution of laboratory sorption experiments. The third approach is the post processing of the result data, implementation of mathematical models for the kinetics of sorption and further comparing the results obtained with the experimental results.

Chapter 2 – presents an overview of the state of the art of the existing groundwater flow models is presented. First, the mathematical formulation of flow in saturated and variably saturated porous media is recalled, including its associated boundary and

initial conditions and the Richards equation. In the second part the mechanisms of conservative and non conservative contaminant transport in porous media is presented with various variants of the transport equation, emphasis is laid on both the equilibrium and non-equilibrium situations which is widely used in hydrology and waste water treatment.Finally, numerical solution of the transport equation and its coupled modeling difficulties are presented.

Chapter 3 – presents an review of related work carried out by other researchers on *Pb* sorption on different variants of biochar, with a clear picture of proposed trends, sorption mechanisms and observed results.

Chapter 4 describes the material preparations, equipment and experimental setup procedure.

Chapter 5 – presents a detailed discussion of the results obtained from the experiments and mathematical models, the shortcomings emanating from the experiments and its effects on the applied models are also discussed.

Chapter 7 – presents the major conclusions emanating out of the study.

Appendices – shows the the method used in performing the sorption calculations and the optimization procedure used in the determination of the parameters of the mathematical models used in fitting the experimental data.

Bibliography.bib – contains all the bibliographic information and references that was cited in the thesis.

Chapter 2

Theoretical Concepts

2.1 Governing Equations for Water Movement in Porous Media

Water on the subsurface is generally divided into two main types:the phreatic water or soil moisture in the variably saturated zone, and groundwater which exists in the saturated zone.The division is mainly due to the differences in the physics of the flow behavior in the saturated and the variably saturated zone.

The zone which exists above the water table - shown in figure (2.1) showing the elevation at which the pressure in the water phase is atmospheric-is denoted as the *vadose zone*.This zone sustains the saturated flow in the capillary fringe and unsaturated flow above the capillary fringe.Below the water table there is the saturated flow, assuming the absence of trapped air or non aqueous phase liquids below the water table. The next section 2.1.1 elaborates further on the equations that describe saturated flow in the subsurface, while the unsaturated flow is addressed in section 2.1.2.This examination will enable the development of models required to simulate subsurface contaminant transport.

2.1.1 Saturated Porous Media flow equation

The governing equation of groundwater flow is the mathematical relationship used to describe the flow behavior in saturated Porous Media media[Anderson, 1992] these mathematical relationships describing groundwater flow is often derived for an infinitesimal representative elemental volume REV whereby the properties of the medium are typically assumed to be effectively constant.

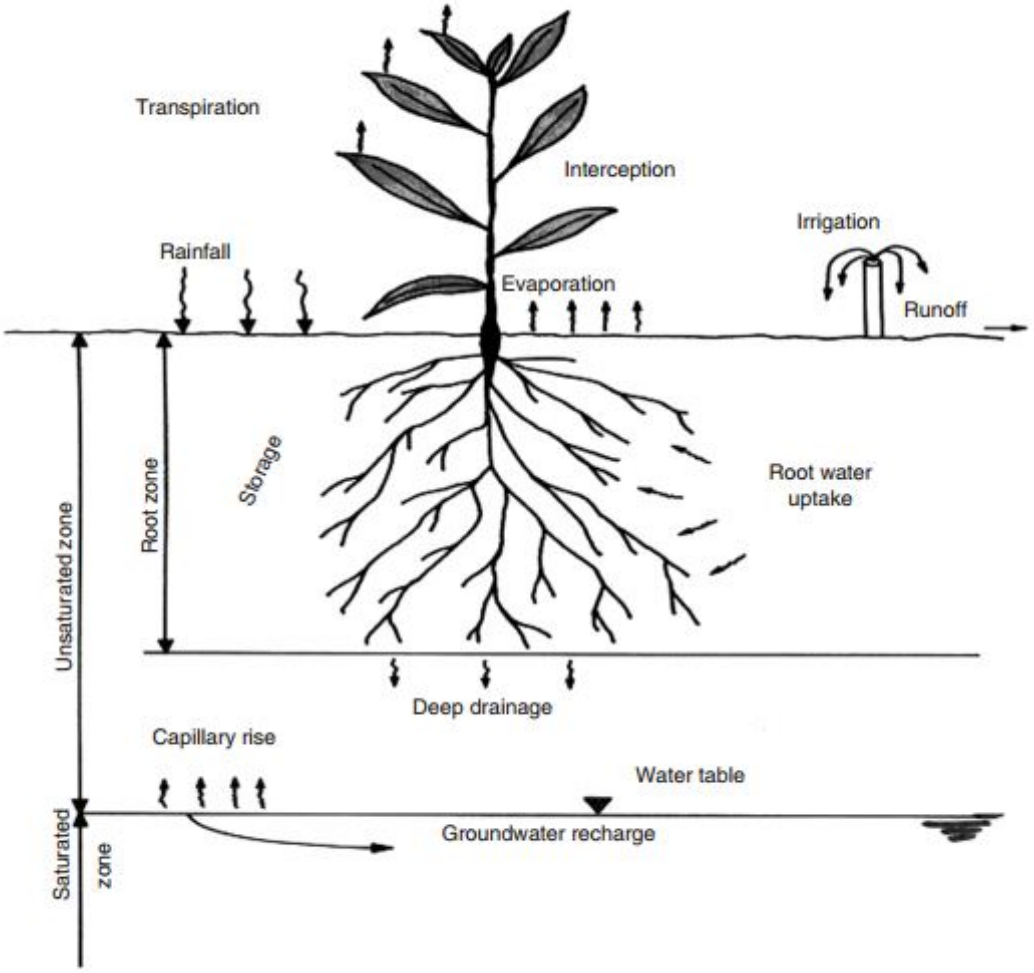

FIGURE 2.1: Distinction between saturated and unsaturated zones[figure from Jirí Simunek, 2006]

The mathematical relationships describing groundwater flow are mainly based on the Darcy's law (equation 2.1) in combination with the mass balance equation (2.2).According to the Darcy's law, the average flow velocity is directly proportional to the hydraulic gradient [Freeze & Cherry, 1979]. The proportionality factor is determined as the hydraulic conductivity.

$$\vec{q} = -\mathbf{K}\nabla H \tag{2.1}$$

$$-\frac{\partial V_f}{\partial t} = \nabla \cdot \vec{q} \tag{2.2}$$

Where V_f is the volume function which is in this case represents the variably saturated moisture content, $\vec{q}$ is the volume flux, t time H, and the total hydraulic head composed of the pressure head h and geodetic head z equation which can be expressed as:

$$H = h + z$$

The vector ∇H is perpendicular to the equipotential surfaces, and based on its definition is oriented from the lower values of the hydraulic head toward the higher values due to the fact that the groundwater flows from the higher head to the lower head, the sign of minus is applied so as to obtain positive values of the discharge thus oriented.

For the case of an isotropic porous media, the vectors $\vec{q}$ and ∇H both have the same direction, but opposite senses; whereas in the case of isotropy, its parallel to the flow lines (fig 2.2a).

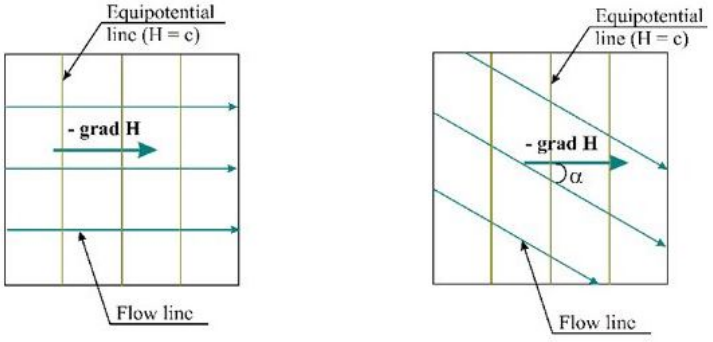

FIGURE 2.2: The oOrientation of flow lines and of the vector ∇H a) isotropic aquifer; b) anisotropic aquifer[figure from Fetter, 2000]

Equation (2.1) is valid only if **K** is an isotropic property of the porous media, independent of the direction. Actually, porous media are stratified and present a strong anisotropy as well. In case of anisotropy, ∇H remains perpendicular to the equipotential surfaces, but the flow lines will cross them at an angle depending on the degree of anisotropy. This means that in this case,∇H is no longer parallel to the flow lines (Figure 2.2).

For the case of an anisotropic porous medium, if the coordinate axes are aligned along the major axes of anisotropy, Then both the volume flux vector $\vec{q}$ and the components of the hydraulic conductivity tensor **K** in three-dimensional space, could be written in matrix form as:

$$\vec{q} = \begin{bmatrix} q_x \\ q_y \\ q_z \end{bmatrix} = \begin{bmatrix} -K_{xx}\frac{\partial H}{\partial x} & -K_{xy}\frac{\partial H}{\partial y} & -K_{xz}\frac{\partial H}{\partial z} \\ -K_{yx}\frac{\partial H}{\partial x} & -K_{yy}\frac{\partial H}{\partial y} & -K_{yz}\frac{\partial H}{\partial z} \\ -K_{zx}\frac{\partial H}{\partial x} & -K_{zy}\frac{\partial H}{\partial y} & -K_{zz}\frac{\partial H}{\partial z} \end{bmatrix} = -\mathbf{K}\nabla H \tag{2.3}$$

A mathematical relationship Similar to equation (2.3) could be obtained in the case of two-dimensional space, vanishing the 3rd component. Thus, in the case of a two-dimensional horizontal system, the combination of the Darcy's law (2.1) with the continuity equation (2.1)(2.2) yields the general form of the transient groundwater flow equation (2.4):

$$\vec{q} = \begin{bmatrix} q_x \\ q_y \end{bmatrix} = - \begin{bmatrix} K_{xx} & K_{xy} \\ K_{yx} & K_{yy} \end{bmatrix} . \begin{bmatrix} \frac{\partial H}{\partial x} \\ \frac{\partial H}{\partial y} \end{bmatrix} = -\mathbf{K}\nabla H \tag{2.4}$$

H is the piezometric (hydraulic) head and K_{xx}, K_{yy} are the hydraulic conductivities along the x, y axes which are assumed to be parallel to the major axes and needed to be defined everywhere within the domain to which the equation applies [Pinder & Celia, 2006]

2.1.2 Variably Saturated Porous Media flow equation

The vadose (unsaturated) zone could be described as the layer between the land surface and the permanent or seasonal groundwater table. While the pores in-between the solid grains are fully filled with water in the saturated zone (groundwater), pores in the Variably Saturated zone remains only partially filled with water, with the rest of the pore space occupied by gaseous phase. Although saturated regions may exist, the vadose zone is mostly only partially saturated,for example when perched water is present above a low-permeable fine textured (clay) layer or if a saturated zone is behind the infiltration front during or after a high intensity rainfall event.

As contaminant transport is closely associated with the water flux in soils making up the vadose zone, any quantitative analysis of contaminant transport must first evaluate water fluxes into and through the vadose zone. the Water usually enters the vadose zone in the form of irrigation or precipitation (Figure 2.1) or by means of industrial spills. due to the close relationship between water flow and solute transport,the physics and mathematical description of variably saturated flow in porous media will be the primary

focus of this section,which would be followed by a discussion of the governing solute transport equations in Section 2.4.

The Richards equation gives the descriptions of variably saturated flow in porous media, it combines the Darcy–Buckingham equation (2.8) for the fluid flux with the mass balance equation (2.5). The governing equation of groundwater flow has a diffusion term and an advection term which is related to gravity and only acts in the z-direction.

When the soil is fully saturated, all pores are filled with water and participate in the transport of water, but When the soil is unsaturated the water movement takes only place through thinner and thinner pores using more tortuous ways. As a result of this, the unsaturated hydraulic conductivity is not a constant, rather varies non-linearly with the volumetric water content: $K = K(\theta)$. The relationship between K and θ can be determined experimentally.

The time rate of change of mass of water in the control volume per unit area of soil could be given as:

$$-\frac{\partial \theta}{\partial t} = \nabla \cdot \vec{q} \tag{2.5}$$

Darcy law for unsaturated flow can be expressed as:

$$\vec{q} = -\mathbf{K}(h).\nabla H \tag{2.6}$$

where K_s is the tensor of unsaturated hydraulic conductivity,$\vec{q}$ is the darcy volume flux, θ is the water content, and t is time.

In unsaturated flow the void spaces are partially filled with water so that water is attracted to the particle surfaces [Mays, 2010].This in turns draws water up around the particle surfaces,leaving behind air in the center of the voids.The energy due to the soil suction forces is refered to as the *pressure head* h in unsaturated flow,which varies with moisture content and z is the *geodetic head*.Total head is then the sum of the geodetic and pressure heads:

$$H = h + z \tag{2.7}$$

Combining with equation (2.6),we obtain the Darcy–Buckingham Equation:

$$\vec{q} = \mathbf{K_s}(h)(\nabla h + \begin{bmatrix} 0 \\ 0 \\ 1 \end{bmatrix}) \tag{2.8}$$

Substituting $\vec{q}$ from the equation (2.8) above in the continuity equation (2.5) we get:

$$\frac{\partial \theta(h)}{\partial t} - \nabla \cdot \mathbf{K_s}(h)\nabla h - \frac{\partial \mathbf{K_s}(h)}{\partial z} = 0 \tag{2.9}$$

We then get the equation above, which is also called the mixed form [Celia *et al.* , 1990] of Richard equation because the equation is parameterized in h but the time-stepping is in terms of θ.

The mixed form of The Richards Equation containing the pressure and the saturation is discussed above. It can also appear in two other formulations: head-based and saturation-based.

As noted in [Celia *et al.* , 1990] the $'head'\text{-}based\ form$ of Richards equation can be written in the continuous form as:

$$\frac{d\theta}{dh}\frac{\partial h}{\partial t} - \nabla \cdot \mathbf{K_s}(h)\nabla h - \frac{\partial \mathbf{K_s}(h)}{\partial z} = 0$$

the $'Saturation'\text{-}based\ form$ of Richards equation can be written in the continuous form as:

$$\frac{\partial \theta}{\partial t} - \nabla \cdot D(\theta)\nabla \theta - \frac{\partial \mathbf{K_s}(\theta)}{\partial z} = 0$$

Where K_s is the unsaturated hydraulic conductivity, h is the pressure head, z is the elevation above a vertical datum, θ is the water content, t is time,$\frac{\partial \theta}{\partial h}$ is the moisture capacity $C(h)$ $[L^{-1}]$ and $D(\theta)$ $[L^2T^{-1}]$ is 'the unsaturated soil water diffusivity': $D(\theta) \equiv \frac{\mathbf{K_s}(\theta)}{C(\theta)} \equiv \frac{\partial h}{\partial \theta}$.

Equation (2.9) provides the basis for predicting transient soil-water movement in layered soils, each layer of which may have different physical properties.

2.1.3 Boundary Conditions

The boundaries of a groundwater flow model are described by the domains or points at which the dependent variable such as the head or the derivative of the dependent flux is known. The boundaries could be inner or outer boundaries. An impermeable body of rock (figure 2.3) or a large body of surface water could form the physical boundary of the groundwater flow systems, while a groundwater divide or streamline could form the hydraulic boundary. [Anderson, 1992] .

A distinct solution requires, at least one distinctive boundary condition is specified. There are two basic types of boundary conditions:

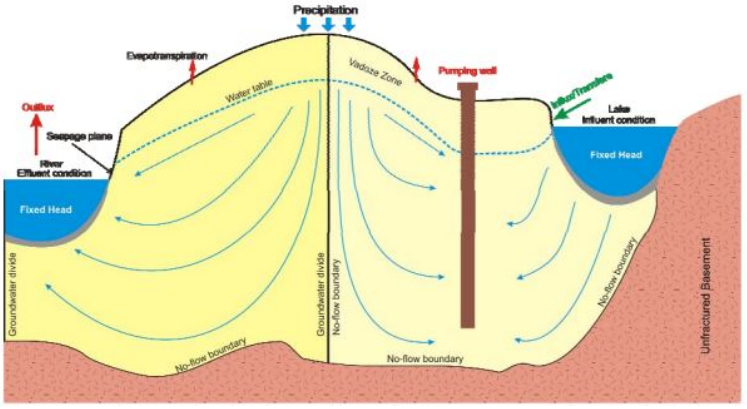

FIGURE 2.3: Illustration of regional groundwater flow system representing physical and hydraulic boundary conditions.[figure from Anderson, 1992]

The **First type or Dirichlet condition** involves the provision of known values of the hydraulic head by the boundary and the source of water with a constant water level at the model boundary. This kind of condition is used to model an aquifer which is in good interaction with a river, lake or other external aquifer. it occurs mostly where the groundwater is in direct contact with the surface water such as a lake or a river and interact freely with the aquifer. it is mathematically given as:

$$h(x,t) = h_0 \qquad \forall (x,t) \in \partial\Omega_1 \qquad X[T_{init}, T_{end})$$

where t is the time $[T]$, h_0 is the specified boundary values of hydraulic head h along the boundary segment $\partial\Omega_1$ of the overall domain $\partial\Omega$

The **Second type or Neumann condition** requires the specification of water fluxes by a boundary. A no-flow boundary (where the water flux is zero) is the most popular Neumann boundary condition. Several types of specified flux conditions exists such as the impermeable boundaries that allow zero flux, the recharge boundaries located at the top of the saturated zone, and wells which are pumped at a known rate.

Mathematically the **Neumann** boundary condition is stated as follows:

$$\frac{\partial h(x,t)}{\partial \vec{n}} + n_z = 0, \qquad \forall (x,t) \in \partial\Omega_2$$

Where n_z is is the vertical component of boundary segment normal vector

The flux across the boundary is already known. It includes a no flow boundaries between boundaries where the flux is specified to be zero, interactions between groundwater and surface water bodies, spring flow and underflow. The most frequently applied form of a Neumann Boundary is a No-flow boundary, which typically occurs between a highly permeable area and an area of much lower permeability or from a water divide.

2.1.4 Initial Conditions

The equation (2.9) contains a term of the first order time derivative.Thus it becomes necessary from a mathematical perspective to define the state of the system at the beginning of the simulation period.

The pressure head distribution everywhere in the system at the beginning of the simulation forms the initial conditions; thus, they represent the boundary conditions at the first time step.While for the case of a steady state model the heads could be estimates or averages of all the data available; however, in he case of transient models the pressure heads could be real values or the result of a steady state simulation.
Problems of Steady state requires at least one boundary node with a known head so as to give the model a reference elevation from which to calculate heads.While in transient situations the initial conditions provides the reference elevation of the head solution and is expressed by the following equation:

$$h(x, t_0) = h_0(x), \ \forall x \in \Omega$$

where $h_0(x)$ is a spatially varying initial head distribution and t_0 the initial time.

2.2 Mechanisms of Solute Transport in Porous Media

Contaminant transport in porous media do requires an understanding of the chemical and physical factors that can interact between themselves,such as sorption, dispersion, degradation, or chemical reactions,which could possibly affect its movement through the groundwater and its prediction.

2.2.1 Concept of Pore Water Velocity and Effective Porosity

A geological medium is said to be any type of rock or sediment in the subsurface.If he flow of groundwater occurs along the pore spaces between the rock grains or sediment, that geological medium could be considered to be a porous medium [Makuch, 2004].Examples of porous media are sandstone, gravel and sand aquifers. The flow of groundwater through a porous medium, may involve the choice of different pathways for individual particles of water around the grains of a geological medium (Figure 2.4).

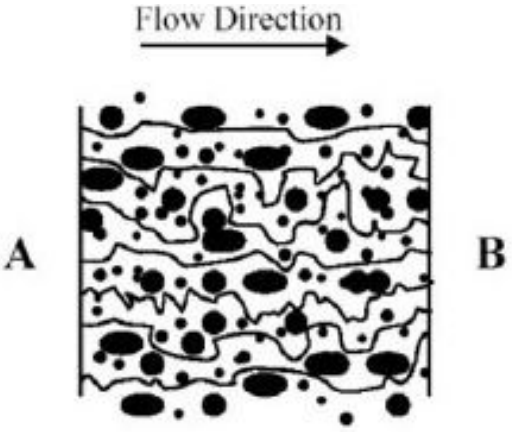

FIGURE 2.4: Various pathways along a porous geological medium.With average linear groundwater velocity being the straight-line distance traveled from A-B divided by the average time required to travel this distance by all water particles[figure from Makuch, 2004]

This pore water velocity, $\vec{v_*}$, could also be known as seepage velocity or interstitial velocity[Manuel Alejandro Salaices Avila, 2009], which defines the average velocity of the water through the porous space and is expressed as:

$$\vec{v_*} = \frac{\vec{q}}{\phi}$$

Where $\vec{q}$ is the Darcy velocity or the specific discharge.In column experiments the volumetric discharge, Q, and the cross section area of the column are known.The pore water velocity, $\vec{v_*}$, is calculated with:

$$\vec{v_*} = \frac{\vec{q}}{\phi} = \frac{Q}{\phi A}$$

The effective porosity, ϕ is known as the section of pore space in a saturated porous media in which the water flow occurs.In other words,it represents the volume of the interconnected voids of a sample.This definition is based on the fact that the entire pore space of a porous medium which is filled with water is not open for water flow.In this thesis, ϕ will denote the effective porosity.

2.2.2 Advective Transport

Advection describes the chemical movement via groundwater flow due to the groundwater hydraulic (i.e. head) gradient[Fetter, 2008]. The solute transport is at the same velocity as that of the fluid flows. Recall that the average linear velocity $\vec{v_*}$ of groundwater flow could be determined from Darcy's law (equation 2.1) For most of the practical problems concerning the transport of contaminant in groundwater, the advection term dominates.To measure the extent of the domination of advection, a dimensionless Peclet number is usually used.The Peclet number is defined as:

$$P_e = \frac{\vec{q} \cdot L}{2 \cdot \mathbf{D}}$$

Where, L is the length of discretization element and $\mathbf{D}$ is the dispersion coefficient.

In problems dominated by advection, known as sharp front problems, the Peclet number has a large value.While for pure advection problems, the Peclet number becomes infinite.

2.2.3 Molecular Diffusion

Molecular Diffusion involves the spreading of a component that is dissolved in the water phase by Brownian motion of the molecules/ions.The transport mechanism behind the phenomenon is called $diffusive\ transport$.

The transport of solutes by diffusive process in a porous medium tends to decrease the existing concentration gradients and could occur in fluids at rest or in the absence of flow of the solution Batu [2006].If the solution is flowing,diffusive transport can still occur and become part of hydrodynamic dispersion along with mechanical dispersion(see Section 2.2.4).

2.2.4 Mechanical and Hydrodynamic Dispersion

The **Hydrodynamic dispersion**, **D**, is the sum of the molecular diffusion and the mechanical dispersion[Fetter, 2008]. It occurs mostly on a larger scale than a single pore, and is usually caused by all variations in the average groundwater velocity (i.e., mean valued over a large number of pores) that was not accounted for explicitly, including diffusion (see figure 2.5).

The hydrodynamic dispersion could occur in the longitudinal or tranversal section,but most atimes the longitudinal component dominates i.e.parallel to the direction of flow, which is represented [see Fetter, 2008]. Longitudinal dispersivity is applied in the approximation of the spreading of the solute concentration in groundwater due to the irregular shape of the interconnected pore space and the variation in velocity at the microscopic level as well as the unresolved macroscopic level.

The groundwater velocity varies according to the size of the pores and the water moves faster at internal points between soil grains than on the solid surface. This spreading is often referred to as **Mechanical dispersion** which occurs in all three spatial directions due to its velocity dependence, it is controlled by the characteristics of the rock layer such as variations in pore size, variations in path length and friction on pore walls (see figure 2.6) thereby causing the invading solute-containing water to transport at different rates, while the mixing that occurs perpendicular to the fluid flow direction is termed **transverse dispersion**. Transverse dispersion is thought to be the result of the division of flow paths to the side (see figure 2.7).

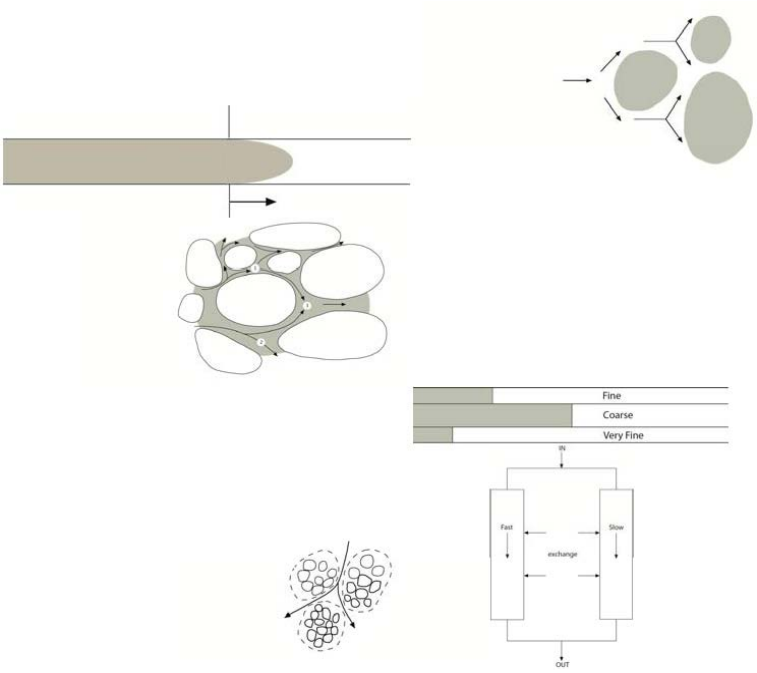

FIGURE 2.5: . Illustration of the different mechanisms of dispersion process. Mixing occurs due to velocity variations within the pores, and between pores, in connection with diffusional mixing at points where water flowing with different concentrations meet. In addition to this, the flow velocities may be aligned in the mean flow direction, but it could also have components situated at an angle with this direction. Also large scale variations in the flow velocity, due to aggregation and layering, may result in enhanced mixing.[figure lifted from der Zee & Leijnse, 2013]

The coefficient of mechanical dispersion is could be described by equation (2.11), where α_i is the dispersivity and v_i is the average linear velocity in the i-direction.

According to der Zee & Leijnse [2013] the longitudinal dispersivity α_i for mechanical dispersion lies in the order of the pore sizes (mm scale) whilein the case of hydrodynamic dispersion, the longitudinal dispersivity depends on the problem scale. in laboratory experiments in columns, values less than $1mm$ up to values larger than $1cm$ have been reported. While for field scale experiments values as large as $10m$ have been reported, dependent on the experiment size and the aquifers' heterogeneity in which the experiment was performed.

Based on evaluation of field experiments[der Zee & Leijnse, 2013], assuming that the permeability of the aquifer is homogeneous over the domain of interest, an empirical relationship for the longitudinal dispersivity estimate has been proposed as:

$$\alpha_i \approx 0.0175 L^{1.46} \tag{2.10}$$

L being a characteristic length for the domain of interest. Based on the assumption that the aquifer permeability remains homogeneous over the domain of interest. As a guideline, the transversal dispersivity could commonly be assumed to be 5 to 10% of the longitudinal dispersivity.

$$\text{Mechanical dispersion } = \alpha_i.v_i \tag{2.11}$$

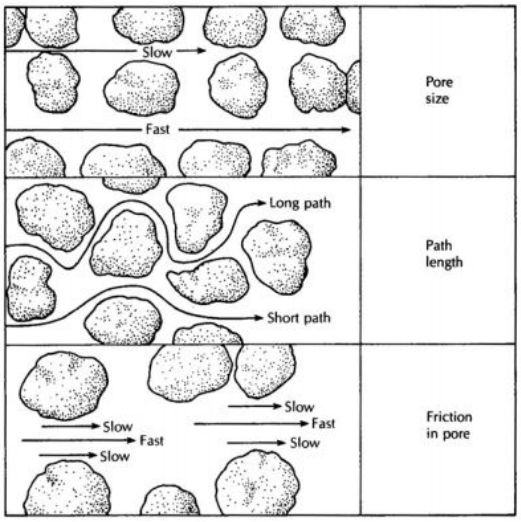

FIGURE 2.6: Factors causing pore-scale longitudinal dispersion[from Fetter, 2008].

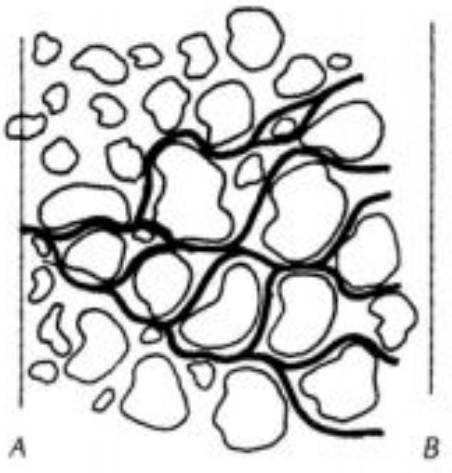

FIGURE 2.7: Flow paths in a porous medium that cause transverse dispersion[from Fetter, 2008].

Since pure mechanical dispersion does never exist [Domenico & Schwartz, 1997] molecular diffusion cannot be separated from mechanical dispersion in flowing groundwater,

the two are combined into a parameter called **hydrodynamic dispersion coefficient**, **D**:

$$\mathbf{D} = \alpha \cdot |\vec{q}| + D^* \cdot I \tag{2.12}$$

Where, I is an identity matrix.

2.3 Chemical Reactions (Nonconservative Solute Transport)

2.3.1 External Reactions

2.3.1.1 Solute Sorption Mechanisms

During adsorption, ions and molecules in water will concentrate on the surface of a solid [Cunha & Nunes, 2011]; the solute being adsorbed is the adsorbate, while the adsorbing solid is the adsorbent.The adsorbates may interact physically with the adsorbent only when the forces of attraction or van der waals forces between the molecules are weak.The adsorbate is not usually fixed to specific sites on the surface of the solid, being free to move over the surface.The adsorption is quite reversible,with the amounts adsorbed being in constant equilibrium with the soluble phase.

Adsorbates which interact by chemical adsorption (also known as chemisorption) with the adsorbent are usually bonded by much stronger forces, similar to those which lead to the formation of chemical compounds.These forces acts as a restraint on the movement of the adsorbate over the solid surface, in such a way that in chemical sorption the solutes forms a single molecule layer on the solid surface, thus exhausting the sorption capacity of the adsorbent.Such an adsorption is almost irreversible and requires high amounts of energy (high temperatures) to free the adsorbed solutes.

Adsorbates could also get adsorbed to solid surfaces due to the forces of electrical attraction.i.e, when the solid surface has acive sites with opposite charge to that of the adsorbent.This mechanism is refered to as an *ion exchange* process.The smaller the radii of the ions and the larger the charge, the stronger is the attraction.

Adsorption as a surface process is strongly dependent on the solid's surface reactivity and their surface area - adsorption capacity.At the value of the pH usually found in soils, the

adsorption tends to be essentially cationic.The number equivalents of cations retained by the soil by exchangeable adsorption (i.e.,physical adsorption and ion exchange) is refered to as its cation exchange capacity (CEC).

Observations from experimental studies shows that the capacity of a solid to remove a solute is a function of the solute concentration. The plot which shows the relationship between the amount of solute sorbed onto the solid (c^*) and the concentration (c) of the solute is called an isotherm. When the process of sorption is very fast compared to the velocity of water flow in the porous media, the sorption process will tend toward an equilibrium state, which is described by an equilibrium sorption isotherm. On the other hand, when the process of sorption is much slower compared to the flow velocity of water in the porous media, then equilibrium conditions won't be reached..In such a situation a kinematic sorption model becomes necessary to model the sorption phenomenon. In the next sections, the various isotherms that are used to model the equilibrium and kinematic sorption model will be discussed.

2.3.1.2 Equilibrium Sorption

Equilibrium is attained when the capacity of the adsorbent material has been reached.The theoretical sorption capacity or equilibrium sorption of the adsorbent is described by a sorption isotherm, which shows the relationship between the amount of metal ion sorbed and the equilibrium concentration of metal ion in the soil solution.

If a linear relationship is obtained over the concentration range studied then the sorption process could be described by a single coefficient, the distribution coefficient, K_d.For metals, however,the relationship is hardly ever linear and other equations with two or more coefficients must be used to describe the data.

The relationship between the adsorped and dissolved solute concentrations may be described using three possible isotherms: linear, freundlich and langmuir.

The significance of such isotherms is that they show how the adsorbate molecules (metal ion in aqueous solution) are distributed between the solution and the adsorbent solids at equilibrium concentration.

Linear Sorption Isotherm

The linear sorption reaction considers that the solute concentration sorped to the porous medium is directly proportional to the reaction as shown in Figure 2.8. The linear model assumes there is no competition between molecules of the chemical species,i.e., that there is a large surplus of adsorped, and the adsorption is propotional to the concentration

in the solution.Such adsorption behavior would only be possible if the rate between the total amount of molecules in solution and the amount of available sites for adsorption is very low.

The linear equilibrium isotherm is mathematically expressed as,

$$c^* = K_d c \tag{2.13}$$

Where,
$K_d[M^{-1}L^3]$ is the distribution coefficient.
c^* = mass of solute sorbed per dry unit weight of solid $[M^{-1}L^3]$
c = concentration of solute in solution at equilibrium with the solid $[M^{-1}L^3]$

the linear sorption isotherm has two main drawbacks. The first one is that the relation between c^* and c is linear (which may not be the actual case) and there is an upper limit on c^*, i.e. there is an upper limit to the mass of solute that can be sorbed onto the solids.

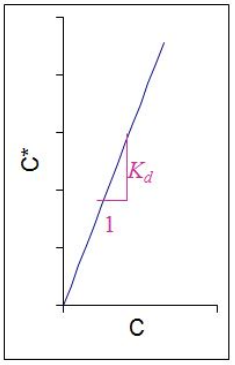

FIGURE 2.8: Linear Sorption Isotherm with c^* vs c

Freundlich Sorption Isotherm

The competition for adsorption sites increases as the rate increases, resulting in an adsorption process which is less than propotional.Isotherms of this process are modeled by *Freundlich Sorption models*. Freundlich isotherm typically describe the adsorption characteristics for the heterogeneous surface.

The non-linear Freundlich equilibrium isotherm (Figure 2.9) could mathematically be expressed as,

$$c^* = K_f c^N \tag{2.14}$$

Where,
$K_f[M^{-1}L^3]$ Freundlich constant related to maximum adsorption capacity (mg/g). It is a temperature-dependent constant.
N = Freundlich contestant related to surface heterogeneity (dimensionless). It gives an indication of how favorable the adsorption processes. $[M^{-1}L^3]$.

The plot of c^* versus c yields a non-regression line permiting the determination of (N) and K_f .Values of N ranges between 0 to 1, where the closer the value is to zero means the more heterogeneous the adsorption surface.On linearization, these values can be obtained by plotting $(logc^*$) versus $(logc$) as presented in equation (2.15).From the plot, the vales K_f and N can be obtained.

The Freundlich equilibrium isotherm overcomes one of the main drawbacks of the linear equilibrium isotherm. But, couldn't overcome the second disadvantage that there exist an upper limit to the mass of solute that can be sorbed onto the solids.

$$\log c^* = \log K_f + N \log c \tag{2.15}$$

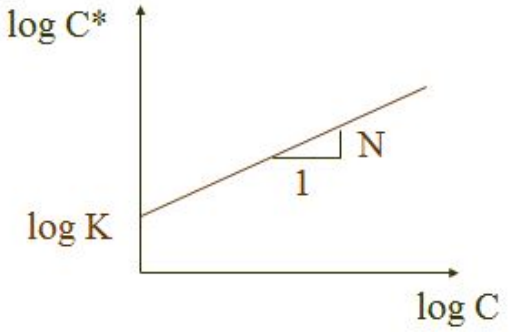

FIGURE 2.9: Freundlich Sorption Isotherm (a) Normal scale (b) Log-Log scale

Langmuir Sorption Isotherm

The Langmuir adsorption isotherm describes quantitatively the formation of a monolayer of adsorbate on the outer surface of the adsorbent [Al-Anber, 2011], after that no more

adsorption takes place. Thus, the Langmuir represents the equilibrium distribution of metal ions between the solid and liquid phases.

It is based according to the assumption that every adsorption site is similar and energically equivalent (thermo dynamically, each site can possibly hold one adsorbate molecule). The Langmuir isotherm postulates that the ability of molecule to bind and be adsorped is not dependent of whether or not neighboring sites are occupied.

The Langmuir Sorption Isotherm can be expressed mathematically as,

$$\frac{c}{c^*} = \frac{1}{\alpha\beta} + \frac{c}{\beta} \tag{2.16}$$

Where,
α is a constant representing the degree of adsorption affinity to the adsorbate,
β is the maximum amount of solute that can be adsorbed by the soil surface.
High value of α indicates for much stronger affinity of metal ion adsorption.

$$\frac{c}{c^*} = \frac{1 + \alpha c}{\alpha\beta} \tag{2.17}$$

$$c^* = \frac{\alpha\beta c}{1 + \alpha c} \tag{2.18}$$

A plot of $\frac{c}{c^*}$ versus c gives a straight line of slope $\frac{1}{\beta}$ and intercept $\frac{1}{\alpha\beta}$,as shown in figure (2.10).

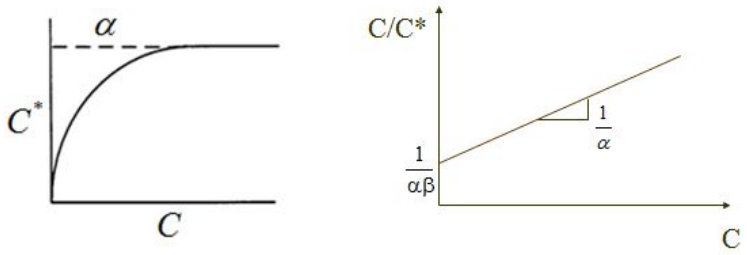

FIGURE 2.10: Langmuir Sorption Isotherm (a) c^* - c plot normal scale (b) c - c/c^* plot in scale log - log scale

2.3.1.3 Kinetic Sorption

When the flow velocity becomes high, the sorption process is likely not able to reach the equilibrium state. In such a situation, kinetic model becomes more appropriate. The typical non equilibrium condition is the linear relationship between the rate of sorption and the solute concentration remaining in the solution. The relation can be mathematically represented as,

$$\frac{\partial c^*}{\partial t} = K_1 c \tag{2.19}$$

Where, K_1 is a first order decay rate constant.

The above relation, considers that the sorped process is irreversible so therefore the solute cannot be desorped once its sorped onto the solid surface. However, the sorped process is reversible and the rate of sorption is depends also on the amount of solid already sorbed onto the soil solid.
Taking the reversibility into consideration, the reversible linear kinetic sorption equation can be written as,

$$\frac{\partial c^*}{\partial t} = K_2 c - K_3 c^* \tag{2.20}$$

Where, K_2 is the forward rate constant and K_3 is the backward rate constant.

The system will attain equilibrium condition if sufficient time is made available to the system. Then $\frac{\partial c^*}{\partial t} = 0$

Thus

$$K_2 c = K_3 c^* \tag{2.21}$$

$$c^* = \frac{K_2}{K_3} c \tag{2.22}$$

$$c^* = K_d c \tag{2.23}$$

This is the linear equilibrium sorption isotherm equation (2.13)

The reversible linear kinetic sorption model can also be written as,

$$\frac{\partial c^*}{\partial t} = \gamma(K_4 c - c^*) \tag{2.24}$$

At the equilibrium condition $\frac{\partial c^*}{\partial t} = 0$

Thus,

$$K_5 c^N = K_6 c^* \tag{2.25}$$

$$c^* = \frac{K_5}{K_6} c^N \tag{2.26}$$

This is the Freundich equilibrium sorption isotherm.

The kinetic version of the Langmuir sorption model can as well be written as,

$$\frac{\partial c^*}{\partial t} = K_7 c(\beta - c^*) - K_8 c^* \tag{2.27}$$

Where β is the maximum amount of solute that can be sorbed,K_7 is the forward rate constant and K_8 is the backward rate constant. And this is known as bilinear adsorption model.

2.3.2 Internal Reactions

Internal reactions in solute transport is generally used to describe a solute that decays at a constant rate or undergoes biodegradation.For organic pollutants, degradation remains the key removal mechanism.It typically involves microbes and relatively complex

transformation mechanisms. In many practical cases, however, degradation is modeled as first-order decay.

Due to the decay, the material concentration will reduce both in the dissolved and sorped phase. Moreover,the decay can be modeled as:

$$\left(\frac{\partial c}{\partial t}\right)_{decay} = -\frac{\ln 2}{\lambda} c \tag{2.28}$$

Where, $\frac{\ln 2}{\lambda}$ represents the radioactive half time and λ is the radioactive decay constant.

2.4 Conservative Governing Equation of Solute Transport

2.4.1 Mass Balance on REV

This principle of conservation of mass is extremely useful. It means that if the amount of a contaminant somewhere (say, in a soil) increases, then that increase cannot be the result of some "magical" formation out of nowhere. The contaminant must have been either carried into the soil from elsewhere or produced via chemical reaction from other compounds that were already in the soil. And, if chemical reactions produced the mass increase in our contaminant, they must also have caused a corresponding decrease in the mass of some other compounds. Thus, conservation of mass allows us to compile a budget of the mass of our contaminant in the soil. This budget keeps track of the amounts of contaminant entering the soil, leaving the soil, and the amount formed or destroyed by chemical reaction. This budget can be balanced for a given time period.

A mass balance requires that the total flux into the REV is equal to the change of stored mass in the REV.Hence,the sum of flux leaving the volume through the surface (the dot product of the three dimensional flux vector,$\vec{J}$,and the unit normal vector,$\vec{n}$,over the boundary surface,S and sources and sinks within the volume,G,equals the time rate of change in storage of mass inside the REV (figure 2.11)c is the total mass of solute per unit volume in the volume and $\frac{\partial c}{\partial t}$ is the time rate of change of solute mass.This mass balance is given by

$$-\oint_S (\vec{J}.n)\, dS + \int_v G\, dV = \int_v \frac{\partial c}{\partial t}\, dV \tag{2.29}$$

The first term in Equation (2.29) is the mass entering into the volume as a flux through the surface,with a flux across surface into the volume defined as being negative.The second term is the source/sink term or the mass of solute generated or decayed per unit time in volume.The third term on the right-hand side of Equation(2.29) is the time rate of change of mass in the volume.

With the application of the Gauss divergence theorem (equation 2.30),the surface integral in Equation (2.29) could be transformed into a volume integral (equation 2.31).

$$\oint_S (\vec{k}.n)\ dS = \int_v (\nabla.\vec{k})\ dV \tag{2.30}$$

$$\oint_S (\vec{J}.n)\ dS = \int_V (\nabla.\vec{J})\ dV \tag{2.31}$$

By applying equation (2.30) to the flux term from equation (2.29) we get equation (2.32):

$$-\int_V (\nabla.\vec{J})\ dV + \int_V G\ dV = \int_V \frac{\partial c}{\partial t}\ dV \tag{2.32}$$

Bring everything over to one side to get equation (2.33)

$$\int_V \left[(\nabla.\vec{J}) + \frac{\partial c}{\partial t} - G\right]\ dV = 0 \tag{2.33}$$

Since the volume V is completely arbitary, it could be located at any point then everything inside the integral = 0 giving equation (2.34) and rearranging terms to get the *continuity equation* (2.35).where $\vec{j}$ is the total flux.

$$(\nabla.\vec{J}) + \frac{\partial c}{\partial t} - G = 0 \tag{2.34}$$

$$\frac{\partial c}{\partial t} = -(\nabla.\vec{J}) + G \tag{2.35}$$

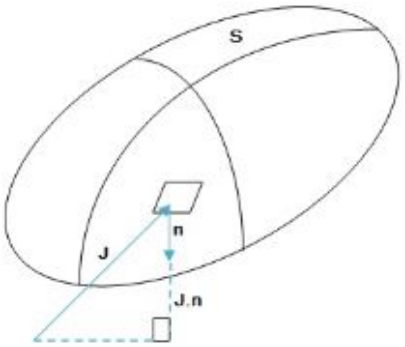

FIGURE 2.11: Mass balance on an REV with parameters J and n,the flux and surface normal vectors respectively.S is the surface of the volume V.

2.4.2 Microscopic Scale Mass Flux

The solute flux in porous media $\vec{J}$ in equation (2.35) comprises three components: $\vec{J}_{dif}$ (diffusive flux), $\vec{J}_{dis}$(dispersive flux), and $\vec{J}_{adv}$ (advective flux).

In open water, the mass flux due to diffusion is given by Fick's first law given in equation (2.36).Where D_m is a scaler known as the *molecular diffusion coefficient*, The -$\nabla.c$ which is a vector quantity is an indication that mass moves from regions of high concentration to regions of low concentration, preferring the direction in which concentration is reduced as quickly as possible.

$$\vec{J} = -D_m.\nabla.c \tag{2.36}$$

the solute mass cannot diffuse as fast as in free water, because the ions or molecules must move along longer pathways through the pore space. To account for this tortuosity effect, an effective diffusion coefficient D^* must be used,which is calculated with the equation (2.37),where τ is the tortuosity of the porous medium and is defined as the ratio of the total length travelled by the fluid through the porous media and the length of the bed in the direction of the flow.According to Freeze & Cherry [1979], τ ranges from 0.5 to 0.01 for laboratory studies of diffusion of non-adsorbed ions in porous media.

$$D^* = \tau.D_m. \tag{2.37}$$

By modifying Fick's first law(equation 2.36),in the presence of the solid phase to account for the tortous path and porosity, the diffusion flux $\vec{J}_{dif}$ in a saturated porous medium is given by the linear function in equation (2.44).Where D^* is the $effective\ diffusion\ coefficient$,and ϕ is the $effective\ porosity$.

$$D^*\phi\frac{\partial c}{\partial \vec{n}}dA = -D^*.\phi.(\nabla.c.\vec{n})dA = (\vec{J}_{dif}.\vec{n})dA \tag{2.38}$$

$$\vec{J}_{dif} = -D^*\phi\nabla.c \tag{2.39}$$

The flux $\vec{J}_{adv}$ due to advection which is the total mass of solute carried across a unit area oriented normal to the bulk fluid motion is given as equation (2.41), where v_* is the $average\ pore\ velocity$ and ϕ is the $effective\ porosity$ which is the portion of pore space in the saturated porous material in which water flow occurs [Batu, 2006] and $\vec{n}$ is the $unit\ normal\ vector\ over\ S\ the\ surface\ area$.

Advective Flux $\vec{J}_{adv}$ which represents the mass / time going through dA:

$$(\vec{v}_*\phi\vec{c})dA = (\vec{J}_{adv}\vec{n})dA \tag{2.40}$$

$$\vec{J}_{adv} = \vec{v}_*\phi.c \tag{2.41}$$

The total microscopic flux,$\vec{J}$,is the sum of both the advective $\vec{J}_{adv}$, and diffusive, $\vec{J}_{dif}$

$$\vec{J} = \vec{J}_{dif} + \vec{J}_{adv} = -D_*\phi\nabla.c + \vec{v}_*\phi c \tag{2.42}$$

The three-dimensional vector,$\vec{J}$,represents the mass flux of solute at a point in space.

2.4.3 Macroscopic Scale Mass Flux

On a macroscopic scale,the solute flux in porous media $\vec{J}$ in equation (2.35) comprises three components: $\vec{J}_{dif}$ (diffusive flux), $\vec{J}_{dis}$(dispersive flux), and $\vec{J}_{adv}$ (advective flux).

$$\vec{J} = \vec{J}_{dif} + \vec{J}_{adv} + \vec{J}_{dif} \tag{2.43}$$

Solute particles carried by the fluid will travel with a velocity either faster or slower than the average fluid velocity depending on on the particlar flow path followed.To introduce dispersion in the solute transport equation we consider how the velocity variations cause the solute to be transported down gradients at different rates.The dispersive flux can be described by an equation similar to the equation for diffusive flux,given by equation (2.44)

$$\vec{J}_{dis} = -\mathbf{D}^*\phi\nabla.\mathbf{c} \tag{2.44}$$

Where $\mathbf{D}^*$ is the *dispersion coefficient*, and is a second order tensor.Even if flow is isotropic, $\mathbf{D}^*$ is always anisotropic.Dispersion in the longitudinal direction(in the direction of flow) is always much greater than in the tranverse direction.It is usually possible to align the coordinate system (and thereby $\mathbf{D}^*$) in the direction of flow, so that $\mathbf{D}^*$ is symmetric with no off-diagonal components.

Total flux may now be written by substituting the microscopic flux in equation (2.42) and the dispersive flux in equation (2.44) into equation (2.43).

$$\vec{J} = \vec{J}_{adv} + \vec{J}_{dif} + \vec{J}_{dis} = \vec{v}_*\phi c - D_*\phi\nabla.c - \mathbf{D}^*\phi\nabla.c \tag{2.45}$$

$$\vec{J} = \vec{v}_*\phi c - (D_* + \mathbf{D}^*)\phi\nabla.c \tag{2.46}$$

$$\vec{J} = \vec{v}_*\phi c - \mathbf{D}\phi\nabla.c \tag{2.47}$$

where, **D**, the dispersion coffiencient is given as

$$D = D_* + D^* \tag{2.48}$$

D is a tensor term and can be expanded as seen in equation below

$$\mathbf{D} = \begin{bmatrix} D_{xx} & D_{yx} & D_{zx} \\ D_{xy} & D_{yy} & D_{zy} \\ D_{xz} & D_{yz} & D_{zz} \end{bmatrix}$$

By aligning **D** with the velocity we get the simplified equation shown below

$$\mathbf{D} = \begin{bmatrix} D_{xx} & 0 & 0 \\ 0 & D_{yy} & 0 \\ 0 & 0 & D_{zz} \end{bmatrix}$$

By taking the two transverse dispersions D_{yy}, and D_{zz} to be equal, we get an even more simplified equation shown below

$$\mathbf{D} = \begin{bmatrix} D_L & 0 \\ 0 & D_T \end{bmatrix}$$

Where, $\mathbf{D}_L$ and $\mathbf{D}_T$ are the longitudinal and tranverse dispersion coffiencient respectively.

2.4.4 Solute Transport Equation in Saturated Porous Media

Substituting equation (2.47) into (2.35) gives the 3-dimesional advection-dispersion equation (2.49)

$$\frac{\partial c}{\partial t} = -\phi \vec{v}_* \nabla . c - \mathbf{D} \phi \Delta c \tag{2.49}$$

The advection-dispersion equation may be solved analytically or numerically under different initial and boundary conditions.

The numerical approach of the ADE for different boundary conditions will be discussed in the section 2.6

2.4.5 Boundary and Initial conditions

As is evident from equation (2.49),the ADE has second-order partial derivatives.Such second-order equations require that information be provided about the behavior of the dependent variable (in this case concentration),or its derivative,everywhere on the perimeter of the domain in which the governing equation is to be solved.These additional data are refered to as *boundary conditions*.

If the model is two dimensional, boundary conditions must be specified around the one-dimensional line perimeter, in the case of a three-dimensional model,boundary conditions must be specified along the two-dimensional surface that defines the boundary of the domain.If the domain is denoted by Ω, the boundary is often denoted by the symbol $\partial\Omega$.

Boundary conditions for solute transport can be defined similar to the boundary conditions for groundwater flow. We distinguish two types of boundary conditions:

Dirichlet: In this case the concentration on the boundary is fixed. In a flow model, a Dirichlet boundary is a specified-head boundary which acts as a source or sink of water entering or leaving the simulated domain. Similarly, a specified-concentration boundary in a transport model acts as a source providing solute mass to the domain, or as a sink taking solute mass out of the simulated domain. It is often applied at inflow boundaries, where the concentration of the solute in the water phase is known.

Mathematically the **Dirichlet** boundary condition is stated as follows

$$c(x,t) = c_0(x,t) \qquad \forall x \in \partial\Omega_1 \tag{2.50}$$

Where c_0 is the specified concentration along the boundary segment $\partial\Omega_1$ of the overall domain $\partial\Omega$

Neumann: The total mass flow of a solute across a boundary is defined. This type of boundary condition is often applied to inflow boundaries where the total mass of solute entering the groundwater is known (or can be estimated). For outflow boundaries, this type of boundary condition is physically not possible, because at outflow boundaries the total mass leaving the system is unknown (dependent on the concentration in the porous media).

Mathematically the **Neumann** boundary condition is stated as follows

$$\frac{\partial c(x,t)}{\partial \vec{n}} = \frac{\partial c(x,t)}{\partial \vec{n}}|_0 \qquad \forall x \in \partial\Omega_2 \tag{2.51}$$

Where $\frac{\partial c(x,t)}{\partial n}|_0$ is the specified outward normal gradient along the boundary segment $\partial\Omega_2$

Initial conditions becomes neccessary due to the presence of a first-order derivative term in equation (2.49).Thus it is necesary, from mathematical perspective,to define the state of the sytem at the begining of the analysis period.Because the dependent variable is the concetration, one is required to specify the concentration everywhere in ω at the initial time t_0, or after a period of time t_n.The initial condition can be written as

$$c(x,t) = c_0(x) \qquad \forall x \in \partial\Omega \tag{2.52}$$

2.5 Non-Conservative Governing Equation of Solute Transport

The differential equations presented in section 2.4 are based on the assumptions that a mass transfer for a solute constituent does not exist between the liquid and solid portions of the groundwater.In this section,the differential equations given in section 2.4 will be modified to include these effects under sorption conditions.

2.5.1 Solute Transport Equation with External Reactions

Sorption is a physical or chemical process by which the solute becomes attached with the soil solids. Sorption processes include adsorption, absorption, chemisorption and ion exchange. The molecules that are sorbed onto the solid are less mobile and they are also not available for phase transfer processes. As a result of the sorption processes, the movement of solute or mixing of solute becomes much slower than the movement of groundwater in an aquifer. Thus sorption induces a retardation effect to the movement of solute in groundwater aquifer. In order to account for sorption effects,modifications to the the solute transport differential equations that are presented in section 2.4 are neccessary.

The advective-dispersion equation given by equation (2.49) for homogenous media, modified to account for the effect of chemical reactions, can be written as

$$\frac{\partial c}{\partial t} = -\phi \vec{v}_* \nabla . c - \mathbf{D}\phi \Delta c - G \tag{2.53}$$

where G is a source-sink term that represents the rate at which the dissolved species is removed from solution.For porous media under sorption conditions, G can be expressed as [see Batu, 2006]

$$G = \frac{\rho_b}{\phi_t} \frac{\partial c^*}{\partial t} \tag{2.54}$$

where c^* is the amount of solute sorbed per unit weight of the solid, ρ_b the dry bulk density of the porous medium,and ϕ_t the total porosity.
Assuming that,

- The chemical processes occur rapidly relative to the flow rate and chemical equilibrium is achieved, and

- Under isothermal conditions the concentration of the solute in the solution is a function only of the concentration in the solid phase,it follows that:

$$\frac{\partial c^*}{\partial t} = \frac{\partial c^*}{\partial c} \frac{\partial c}{\partial t} \tag{2.55}$$

Substitution of equation (2.55) into equation (2.54) yields

$$G = \frac{\rho_b}{\phi_t} \frac{\partial c^*}{\partial c} \frac{\partial c}{\partial t} \tag{2.56}$$

and combining equations (2.53) and (2.56) gives

$$\left(1 + \frac{\rho_b}{\phi_t} \frac{\partial c^*}{\partial c}\right) \frac{\partial c}{\partial t} = -\phi \vec{v}_* \nabla . c - \mathbf{D}\phi \Delta c \tag{2.57}$$

2.5.1.1 Solute Transport Equation under Equilibrium Sorption

Linear Sorption Isotherm

Substituting c^* from equation (2.13) into equation (2.57), the advection-dispersion equation can now be written as,

$$\frac{\partial c}{\partial t} = -\phi \vec{v}_* \nabla . c - \mathbf{D}\phi \Delta c - \frac{\rho_b}{\phi_t}\left(\frac{\partial K_d c}{\partial t}\right) \tag{2.58}$$

$$\left(1 + \frac{\rho_b}{\phi_t} K_d\right)\frac{\partial c}{\partial t} = -\phi \vec{v}_* \nabla . c - \mathbf{D}\phi \Delta c \tag{2.59}$$

$$R\frac{\partial c}{\partial t} = -\phi \vec{v}_* \nabla . c - \mathbf{D}\phi \Delta c [\text{where} R = 1 + \frac{\rho_b}{\phi_t} K_d] \tag{2.60}$$

Where, R$[ML^{-3}]$ is the retardation factor.

Freundlich Sorption Isotherm

Substituting c^* from equation (2.14) into equation (2.57), the advection-dispersion equation can now be written as,

$$\frac{\partial c}{\partial t} = -\phi \vec{v}_* \nabla . c - \mathbf{D}\phi \Delta c - \frac{\rho_b}{\phi_t}\frac{\partial (K c^N)}{\partial t} \tag{2.61}$$

$$\frac{\partial c}{\partial t} = -\phi \vec{v}_* \nabla . c - \mathbf{D}\phi \Delta c - \left(\frac{\rho_b}{\phi_t} K N c^{N-1}\right)\frac{\partial c}{\partial t} \tag{2.62}$$

$$\left(1 + \frac{\rho_b}{\phi_t} K N c^{N-1}\right)\frac{\partial c}{\partial t} = -\phi \vec{v}_* \nabla . c - \mathbf{D}\phi \Delta c \tag{2.63}$$

$$R_f\frac{\partial c}{\partial t} = -\phi \vec{v}_* \nabla . c - \mathbf{D}\phi \Delta c [\text{where} R_f = 1 + \frac{\rho_b}{\phi_t} K N c^{N-1}] \tag{2.64}$$

Where, R_f is the retardation factor for a Freundlich sorption isotherm.

Langmuir Sorption Isotherm

Substituting c^* from equation (2.16) into equation (2.57), the advection-dispersion equation can now be written as,

$$\frac{\partial c}{\partial t} = -\phi \vec{v}_* \nabla . c - \mathbf{D}\phi \Delta c - \frac{\rho_b}{\phi_t} \frac{\partial \left(\frac{\alpha \beta c}{1+\alpha c} \right)}{\partial t} \tag{2.65}$$

$$\left[1 + \frac{\rho_b}{\phi_t} \left(\frac{\alpha \beta c}{(1+\alpha c)^2} \right) \right] \frac{\partial c}{\partial t} = -\phi \vec{v}_* \nabla . c - \mathbf{D}\phi \Delta c \tag{2.66}$$

$$R_m \frac{\partial c}{\partial t} = -\phi \vec{v}_* \nabla . c - \mathbf{D}\phi \Delta c \left[\text{where} R_m = \left[1 + \frac{\rho_b}{\phi_t} \left(\frac{\alpha \beta c}{(1+\alpha c)^2} \right) \right] \right] \tag{2.67}$$

2.5.1.2 Solute Transport Equation under Kinetic Sorption

Substituting equations (2.19), (2.20), into equation (2.57), the advection-dispersion equation can now be respectively written as,

$$\frac{\partial c}{\partial t} = -\phi \vec{v}_* \nabla . c - \mathbf{D}\phi \Delta c - \frac{\rho_b}{\phi_t} K_1 c \tag{2.68}$$

$$\frac{\partial c}{\partial t} = -\phi \vec{v}_* \nabla . c - \mathbf{D}\phi \Delta c - \frac{\rho_b}{\phi_t} (K_2 c - K_3 c^*) \tag{2.69}$$

2.5.2 Solute Transport Equation with Internal Reactions

Substituting c^* from equation (2.3.2) into equation (2.57), the advection dispersion equation with sorption and radioactive decay process can be written as:

$$\frac{\partial c}{\partial t} = -\phi \vec{v}_* \nabla . c - \mathbf{D}\phi \Delta c - \frac{\rho_b}{\phi_t} \frac{\partial c^*}{\partial t} + \left(\frac{\partial c}{\partial t} \right)_{decay} \tag{2.70}$$

$$\frac{\partial c}{\partial t} = -\phi \vec{v}_* \nabla . c - \mathbf{D}\phi \Delta c - \frac{\rho_b}{\phi_t}\frac{\partial c^*}{\partial t} - \frac{\ln 2}{\lambda} c \tag{2.71}$$

2.6 Numerical Modelling of the Solute Transport Equation

Implementation of the numerical modelling of flow and transport in porous media gives approximate solution to the problem,which implies, the unknown variable is solved at discrete points in space (steady-state flow) and time (transient flow). Numerical models are able to solve the more complex equations of multidimensional groundwater flow and solute transport.

The numerical methods for solving the solute transport equation can be classified into three groups[Neuman, 1984]

(I) Eulerian

(II) Lagrangian

(III) Mixed Eulerian-Lagrangian

In the Eulerian approach,the transport equation is discretized by the method of finite differences or finite elements using a fixed mesh,while the lagrangian approach uses a mesh which deforms along with the flow.The mixed approach involves a two-step procedure in which the advective transport is solved using a lagragian approach with concentrations obtained from particle trajectories followed by a subsequent use of Eulerian approach to model the the sinks and sources.

The methods of finite differences and finite elements belong to the first group.These methods were the first numerical methods used for solute transport problems and in spite of their problems discussed below,are still the most often utilized methods.

In this section,a brief descripton of the finite difference and finite elements methods to solve transport problems will be presented.The finite difference method offers a more simplistic approach,while the finite element method has proven to be more suitable for problems involving irregular geometries of the flow an transport problem[Leij *et al.* , 1999], such as flow to drainage pipes and along sloping soil surfaces.

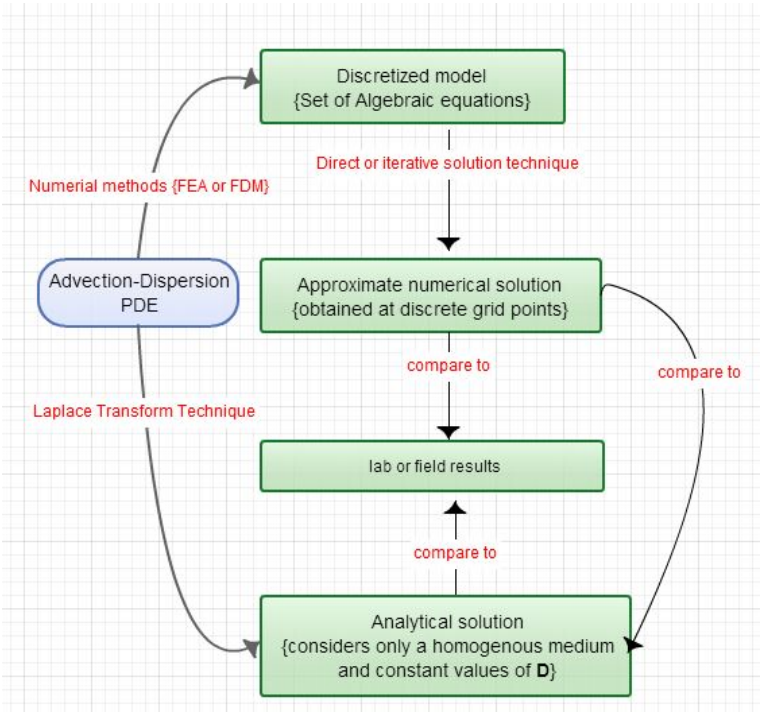

FIGURE 2.12: A flow chart showing the "big picture" of solute transport modeling.

2.6.1 Finite Difference Method (Explicit scheme) of the ADE

The Finite difference method is one of the oldest and most widely used methods for solving differential equations.[UNFAO, 1997].It has a well defined stabiity criterion, meaning that as a general rule, it can be used with confidence knowing fully well that it will yield an accurate solution to the equation being solved.

The differential equation is replaced by a set of finite difference approximations,one for each grid point or node resulting in $n\ x\ m$ simultaneous equations which have to be solved, where n is the number of rows and m is the number of columns of the grid resulting in a matrix.Since most of the elements of the matrix are zero,sparse matrix techniques can be used which require much less computer memory and the added advantage of reducing the computer memory requirements and the time needed to reach a solution.

For steady state problems, the set of equations only needs to be solved once but when a transient problem is involved they need to be solved at every time step. The solution to most partial differential equations cannot be determined analytically. Its often necessary to use Numerical solutions that reduce the problem to algebraic equations which can then be solved by direct or iterative methods.

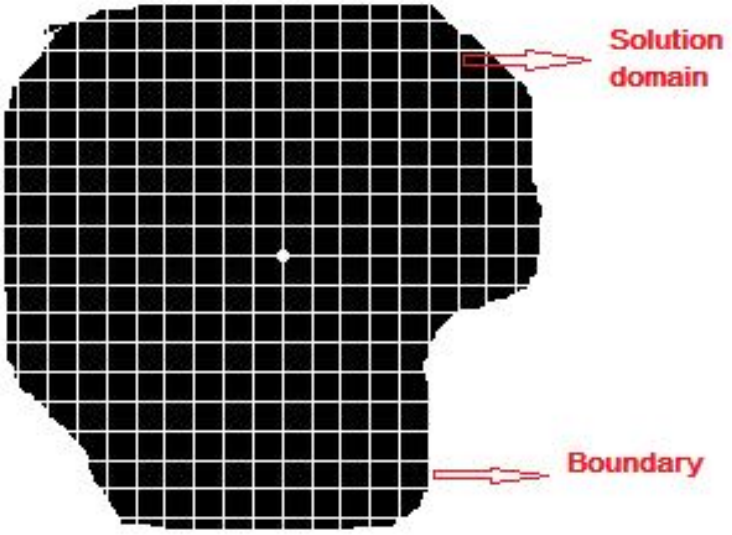

FIGURE 2.13: Regular finite difference grid in 2-dimension.

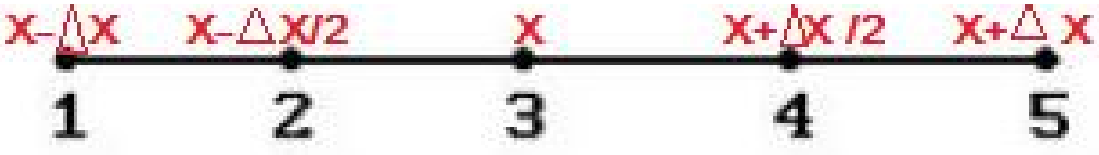

FIGURE 2.14: Grid points in one dimension.

Considering the 1-D grid shown in figure 2.14, The concentration gradient c in the x direction at node 4 would be linearly approximated by

$$\frac{\partial c}{\partial x_{x+\frac{\Delta x}{2}}} \approx \frac{c_{x+\Delta x} - c_x}{x + \Delta x - x} = \frac{c_{x+\Delta x} - c_x}{\Delta x} \tag{2.72}$$

which is a reasonable approximation when x is small enough. Approximation of the second order derivative $\frac{\partial^2 c}{\partial x^2}$ would require obataining a gradient of $\frac{\partial c}{\partial x}$ estimated earlier.Looking in the other direction and computing a gradient at node 2, we obtain

$$\frac{\partial c}{\partial x_{x-\frac{\Delta x}{2}}} \approx \frac{c_x - c_{x-\Delta x}}{x - (x - \Delta x)} = \frac{c_x - c_{x-\Delta x}}{\Delta x} \tag{2.73}$$

Then, taking the gradient between $\frac{\partial c}{\partial x_{x+\frac{\Delta x}{2}}}$ and $\frac{\partial c}{\partial x_{x-\frac{\Delta x}{2}}}$ gives

$$\frac{\partial^2 c}{\partial x^2} \approx \frac{\frac{\partial c}{\partial x_{x+\frac{\Delta x}{2}}} - \frac{\partial c}{\partial x_{x-\frac{\Delta x}{2}}}}{\Delta x} \approx \frac{\frac{c_{x+\Delta x}-c_x}{\Delta x} - \frac{c_x - c_{x-\Delta x}}{\Delta x}}{\Delta x} = \frac{c_{x+\Delta x} - 2c_x + c_{x-\Delta x}}{\Delta x^2} \tag{2.74}$$

A finite difference approximation for $\frac{\partial c}{\partial t}$ is obtained by a forward difference scheme by using the known concentration from the previous time step.At the start of the numerical anaylsis, the initial condition will be the concentration c(t) at t_0.Therefore, we can approximate the derivative $\frac{\partial c}{\partial t}$ by

$$\frac{\partial c}{\partial t} = \frac{c_{x,t} + c_{x,t-\Delta t}}{\Delta t} \tag{2.75}$$

Finally,an expression for the space derivative is required, we had previously used equation 2.72 to develop an expresion for $\frac{\partial^2 c}{\partial x^2}$.It worked well because the result was centered at x.While The first order derivative was centered at $x + \frac{\Delta x}{2}$.To obtain $\frac{\partial c}{\partial x}$ yet with the central finite difference approximation centered at x, we use

$$\frac{\partial c}{\partial x_x} \approx \frac{c_{x+\Delta x} - c_{x-\Delta x}}{2\Delta x} \tag{2.76}$$

The second step involves Replacing the derivative terms in the advective dispersion equation (2.49) with their finite difference approximations obtained in equations (2.74), (2.75) and (2.76) gives

$$-v_* \frac{c_{x+\Delta x,t-\Delta t} - c_{x-\Delta x,t-\Delta t}}{2\Delta x} + D \frac{c_{x+\Delta x,t-\Delta t} - 2c_{x,t-\Delta t} + c_{x-\Delta x,t-\Delta t}}{\Delta x^2} = \frac{c_{x,t} - c_{x,t-\Delta t}}{\Delta t} \tag{2.77}$$

The third and last step is a rearrangement of the discretized equation since nearly all of the concentrations (those with the $t - \Delta t$ subscript) are known from the previous time step or from the initial condition. $c_{x,t}$ is the only exception and it is what we are trying to determine.

rearranging to solve for $c_{x,t}$

$$c_{x,t} = c_{x,t-\Delta t} + \frac{D\Delta t}{\Delta x^2}(c_{x+\Delta x,t-\Delta t} - 2c_{x,t-\Delta t} + c_{x-\Delta x,t-\Delta t}) - \frac{v\Delta t}{2\Delta x}(c_{x+\Delta x,t-\Delta t} - c_{x-\Delta x,t-\Delta t}) \tag{2.78}$$

Because the concentration at the current time step $t - \Delta t$ is known, we can use equation (2.78) to compute the new concentration without solving any additional equations. Such a scheme is called the *explicit* finite difference method and was made possible by the choice to evaluate the temporal derivative with forward differences.

While this explicit method is relatively simple, it is known to be numerically conditionally stable and convergent depending only on the values of the factors $\frac{D\Delta t}{\Delta x^2}$ and $\frac{v\Delta t}{2\Delta x}$. The numerical errors are proportional to the time step and the square of the space step:

$$\Delta c = O(\Delta t) + O(\Delta x^2) \tag{2.79}$$

This can be a serious limitation. There are other approaches that avoid these stability restrictions.

2.6.2 Finite Difference Method (Implicit scheme) of the ADE

In *implicit* finite difference schemes, the spatial derivatives $\frac{\partial^2 c}{\partial x^2}$.are evaluated (at least partially) at the new timestep. In a similar manner as the explicit scheme,The simplest implicit discretization of equation (2.49) is

$$-v_* \frac{c_{x+\Delta x,t} - c_{x-\Delta x,t}}{2\Delta x} + D\frac{c_{x+\Delta x,t} - 2c_{x,t} + c_{x-\Delta x,t}}{\Delta x^2} = \frac{c_{x,t} - c_{x,t-\Delta t}}{\Delta t} \tag{2.80}$$

This can be rearranged so that unknown terms are on the right and known terms are on the left

$$c_{x,t-\Delta t c_{x,t}} = c_{x,t} - \frac{D\Delta t}{\Delta x^2}(c_{x+\Delta x,t} + 2c_{x,t} - c_{x-\Delta x,t}) - \frac{v\Delta t}{2\Delta x}(c_{x+\Delta x,t} + c_{x-\Delta x,t}) \tag{2.81}$$

In this case, there no longer exist an explicit relationship for $c_{x-\Delta x,t}$,$c_{x,t}$,$c_{x+\Delta x,t}$, rather, its necessary to solve a linear system of equations.

Their main advantage is that there are no strict requirements on the timestep, which happens to be good for simulating hydrogeological processes at relatively high spatial resolution. The use of large time steps, however, may result to an inaccurate solution. Therefore it is wise to properly check the results by lowering the timestep until the solution does not change anymore (this is called convergence check).

It is a numerically stable and convergent scheme but it is usually more numerically intensive than the explicit method as it demands solving a system of numerical equations at each time step. The implicit method described in equation (2.83) is second order accurate in space but only first order in time.It is possible also to create a scheme which is both second order accurate in time and in space

$$\Delta c = O(\Delta t) + O(\Delta x^2) \tag{2.82}$$

2.6.3 Crank-Nicolson scheme of the ADE

The Crank-Nicolson scheme is obtained by the computation of the average of both the implicit and explicit schemes of the finite difference method. It generally yields the best performance for diffusion problem, and has a second order accuracy in both time and space, due to the averaging of the explicit and implicit schemes so as to obtain the time derivative which corresponds to evaluating the derivative centered on:

$$-v_* \frac{(1-e)(c_{x+\Delta x,t-\Delta t} - c_{x-\Delta x,t-\Delta t}) + e(c_{x+\Delta x,t} - c_{x-\Delta x,t})}{4\Delta x} \tag{2.83}$$

$$+D\frac{(1-e)(c_{x+\Delta x,t-\Delta t} - 2c_{x,t-\Delta t} + c_{x-\Delta x,t-\Delta t}) + e(c_{x+\Delta x,t} - 2c_{x,t} + c_{x-\Delta x,t})}{2\Delta x^2} = \frac{c_{x,t} - c_{x,t-\Delta t}}{\Delta t}$$

where e is a factor which lies between 0 and 1. For e=1, all the spatial derivatives are determined at the new time (the ending of the time step). This remains a full implicit scheme. For e=0, all the spatial derivatives are determined at the old time (the start of a timestep). It is a full explicit scheme and thus Crank-Nicholsen scheme is obtained by setting e=0.5.

This scheme is almost always convergent and numerically stable but tends to be more numerically intensive since it demands the solution of a system of numerical over both the time and space step:

$$\Delta c = O(\Delta t) + O(\Delta x^2) \tag{2.84}$$

The use of the Crank–Nicolson scheme tends to be the most accurate scheme for smaller time steps. The explicit scheme is remains the least accurate and could become unstable, but its also the easiest scheme to implement whilst being the least numerically intensive. The implicit scheme works the best for large time steps.

2.6.4 Numerical difficulties in solving the ADE

Numerical dispersion is an indication of extra dispersion in numerical solution to the transport equation which is usually caused by discretizing the advective term. UNFAO [1997],the numerical solution usually shows an advancement o the solute at rates greater than is physically possible (see figure 2.16).

Such kinds of errors can not be eliminated completely;they are dissipated during the course of simulation when stable schemes are used,whereas unstable schemes allow such errors to grow.

Implicit schemes shows unconditional stability, however their results may not likely be amenable to variation in grid sizes as this is the case with the explicit systems.The Crank-Nicholson scheme gives a compromise towards unconditional stability, such a property means that, despite other factors, the time step of a variable could be used independently of the space step to adequately balance the requirements of a correct approximation and limited number of computation.However, the oscillations towards the front of the concentration may begin to form also for the unconditionally stable schemes due to a hyperbolic (convection) term in the solute transport equation[Leij *et al.* , 1999]. Finite difference scheme could also be developed to reduce numerical dispersion,however they are likely to cause either an over shooting or undershooting (see figure 2.15) which shows in the numerical solution as oscillations.

There are some standard rules that can pose helpful in reducing the dispersion effects.They use a form of the peclet number, P_e and the courant number, C.

The grid should be disigned such that

$$P_e = \frac{||\vec{q}||\Delta x}{2D} \tag{2.85}$$

Where Δx is the grid size and D_e is the hydrodynamic dispersivity.

The discretization of time should be such that

$$C = v_* \frac{\Delta t}{\Delta x} \tag{2.86}$$

Where v_* being the velocity of flow and Δt the time step is the same as saying that the time step must be less than the time it takes the solute to be advected one grid distance.In the case of a reactive transport solute, the retardation factor has to be added to the denominator of the Courant number.

For an attainment of a stable solution it is thus required that the both conditions are satisfied, meaning that the condition which is the most restrictive would determine the size of the time step size which will still then result in a stable solution.

2.6.5 Finite Element Method of the ADE

The finite element methods is done in very much the same way as the FDM for one-, two-, and three- dimensional problems.One major advantage of the FEM is that they could much be easier used to discretize a complex two- and three-dimensional transport domains. The finite element method follows an integral (as opposed to differential) approach in which the regular grid of the standard FDM has been replaced by an irregular polygonal mesh that allows the modeler to describe different natural shapes more precisely.For ground water the polygonal shape is, most atimes triangular UNFAO [1997].Although quadrilaterals could be used occasionally.A typical finite element grid is shown in (figure 2.17).The intersection point of the triangles is called a node and each of the triangle is called an element.The equation is usually solved by a technique called a weighed residual, the most popular being the Galerkin approach.In this method the weighing functions would be made equal to the basic functions and the integration done over each element and summed to produce the contribution from all the individual elements making up the domain.

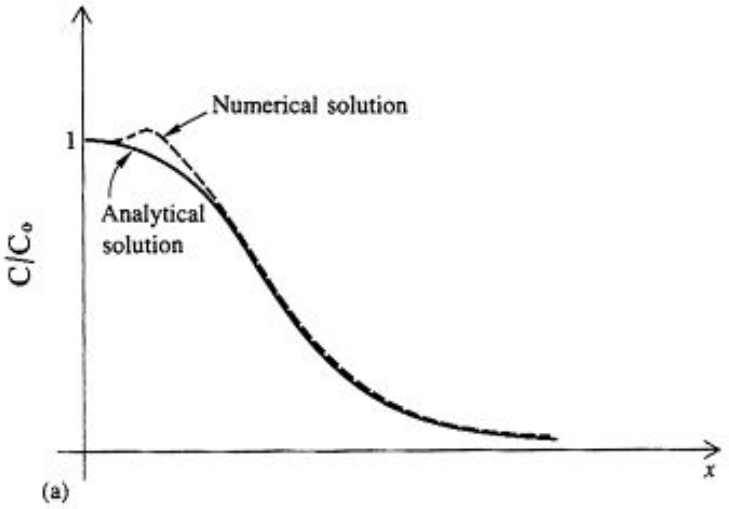

FIGURE 2.15: Effects of overshoot.[Figure lifted from Wang & Anderson, 1995].

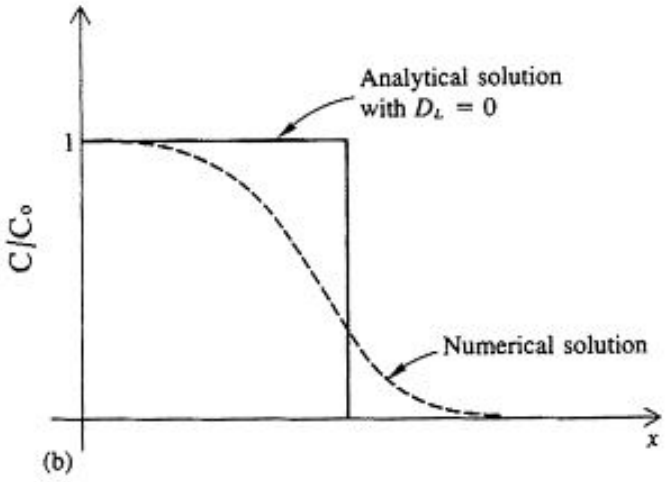

FIGURE 2.16: Effects of numerical dispersion.[Figure lifted from Wang & Anderson, 1995].

$$D_L \frac{\partial^2 c}{\partial x^2} + D_T \frac{\partial^2 c}{\partial y^2} - \frac{\partial v_x c}{\partial x} + \frac{\partial v_y c}{\partial y} = \frac{\partial c}{\partial t} \tag{2.87}$$

The Galerkin method (for detailed explanation of the Galerkin method, please refer to book by Ern & Guermond [2004]) for four-node rectangular elements is applied to the 3-dimensional advection dispersion equation in the principal coordinate axes in equation (2.88).

The residuals of the trial solution $\vec{c}$,weighed by the nodal basis functions $N_L(x, y)$, are set to zero written in the form

$$\oint_S (D_L \frac{\partial^2 c}{\partial x^2} + D_T \frac{\partial^2 c}{\partial y^2} - \vec{v}\frac{\partial c}{\partial x} - \frac{\partial c}{\partial t}) N_L(x,y) dxdy = 0 \tag{2.88}$$

where L=1,2,....,NNODES.

The trial solution within an element ijmn is an interpolation of the nodal nodal values.

$$\vec{c}^e(x,y,t) = N_i^e(x,y)c_i(t) + N_j^e(x,y)c_j(t) + N_m^e(x,y)c_m(t) + N_n^e(x,y)c_n(t) \tag{2.89}$$

The second spatial derivative terms are integrated by parts and the integration over the problem is done element by element.

$$\sum_e \oint_e (D_L \frac{\partial \vec{c}^e}{\partial x}\frac{\partial N_L}{\partial x} + D_T \frac{\partial \vec{c}^e}{\partial y}\frac{\partial N_L}{\partial y} + \vec{v}\frac{\partial \vec{c}^e}{\partial x}N_L + \frac{\partial \vec{c}^e}{\partial t}N_L) dxdy \tag{2.90}$$

$$= \int_L (D_L \frac{\partial \vec{c}}{\partial x} n_x + D_T \frac{\partial \vec{c}}{\partial y} n_y) N_L d\sigma$$

where L=1,2,....,NNODES.

The system of equations represented by equation (2.90) can be written in matrix notation in the form

$$[G]\{c\} + +[U]\{c\} + [P]\{\frac{\partial c}{\partial t}\} \tag{2.91}$$

Where $\{c\}$ is the column matrix of nodal concetrations.and $\{\frac{\partial c}{\partial t}\}$ is The column matrix of the time derivative of nodal concentrations.The square coefficient matrices$[G]$,$[U]$ and $[P]$ corresponds to individual terms in the integral on the left-hand side of equation (2.91).The column matrix $\{F\}$ corresponds to the boundary integral on the right-hand side of equation (2.91).

Typical element matrix entries for the Advective -dispersive equation are

$$G^e_{L,i} = \int_{-a}^{a}\int_{-b}^{b}(D_L\frac{\partial N^e_i}{\partial x}\frac{\partial N^e_L}{\partial x} +_L \frac{\partial N^e_i}{\partial y}\frac{\partial N^e_L}{\partial y})dxdy \tag{2.92}$$

$$P^e_{L,i} = \int_{-a}^{a}\int_{-b}^{b} N^e_i N^e_L dxdy \tag{2.93}$$

The matrix [U] is derived from the advective term $\vec{v_*}\{\frac{\partial c}{\partial t}\}N_L$ in the integrand of equation (2.91).Taking the x derivative of equation (2.89) yields

$$\frac{\partial \vec{c^e}}{\partial x} = \frac{\partial N^e_i}{\partial x}c_i + \frac{\partial N^e_j}{\partial x}c_j + \frac{\partial N^e_m}{\partial x}c_m\frac{\partial N^e_n}{\partial x} \tag{2.94}$$

Therefore, the coefficient which multiplies c_i is

$$U^e_{L,i} = \int_{-a}^{a}\int_{-b}^{b}\frac{\partial N^e_i}{\partial x}N^e_L dxdy \tag{2.95}$$

Similarly, the remaining element matrix terms are

$$U^e_{L,j} = \int_{-a}^{a}\int_{-b}^{b}\frac{\partial N^e_j}{\partial x}N^e_L dxdy \tag{2.96}$$

$$U^e_{L,m} = \int_{-a}^{a}\int_{-b}^{b}\frac{\partial N^e_m}{\partial x}N^e_L dxdy \tag{2.97}$$

$$U^e_{L,n} = \int_{-a}^{a}\int_{-b}^{b}\frac{\partial N^e_n}{\partial x}N^e_L dxdy \tag{2.98}$$

The assembly of the global matrices is perfomed by summation of the element terms.Note that the matrix equation, equation (2.92) has the form

$$[A]\{c\} + [U] + [P]\{\frac{\partial c}{\partial t}\} = \{F\} \tag{2.99}$$

Where $[A]$=$[G]$+$[U]$.The entries of $[G]$ are symmetric in their subscripts.However,the entries to $[U]$ from the advective term,equation (2.95), are not symmetric in their subscripts.The solution to equation (2.99) through time is done by a finite difference approximation for $\frac{\partial c}{\partial t}$.

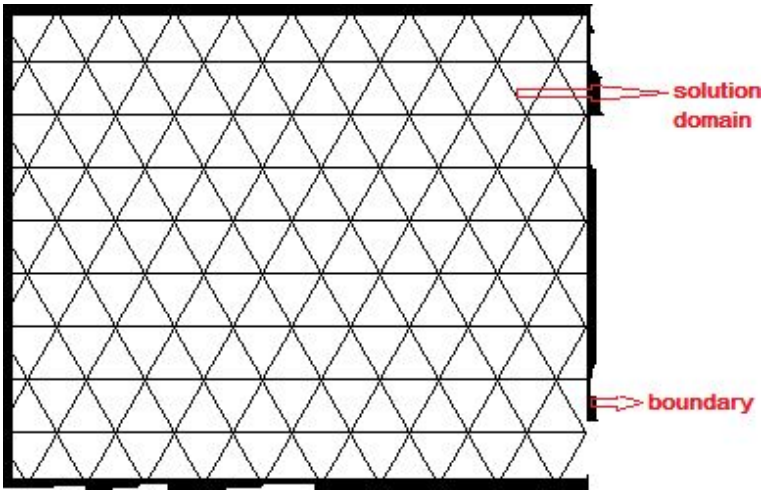

FIGURE 2.17: Typical finite element grid.

Chapter 3

Previous Studies on Metal Sorption and its Mechanisms

Various researchers already utilised a diverse variety of adsorbents to remove heavy metal ions from aqueous solutions.Inline with the scope of this thesis, the review in this section highlights studies carried out with the use of biochar as an adsorbent produced from different agro-biomass and lead (Pb) as adsorbate.
A few of the published recent developments found in literature is shown in table (5.1).

3.1 Effect of biochar on Sorption of Heavy Metal

The sorption of heavy metal to biochar closely affect its bioavailability as well, and the high specific surface area of biochar tends to govern most interactions involving soil and biochar. Usually, this property is greatly influenced mostly by the nature of the agro-biomass material and the conditions under which the biochar is produced such as its pyrolysis temperature [Cao & Harris, 2010]. Table (5.1) summarizes the comparison of $Pb(II)$ sorption capacities (q_t) by various biochars produced from agricultural waste biomass. Grape husks presents relatively higher sorption capacity when compared to 10 other different adsorbents, thus reflecting a promising future for grape husk utilization in Pb ion removal from aqueous solutions.

3.2 Sorption Mechanisms of Biochar

Heavy metal stabilization in soil with the use of biochar could follow different number of pathways such as is illustrated in figure (3.1). In a recent work, Lu *et al.* [2012]

Biochar Feedstock	Pyrolysis temperature (°C)	*pH* (-)	*T* (°C)	c_0 (mM)	*t* (h)	*m* (gL^{-1})	max q_t (mg/g)	Reference
Grape stalks	600	2.0 - 8.0	22	0.1 - 1.5	1 - 48	0.1 - 10.0	595	Trakal *et al.* [2014]
White straws	600	2.0 - 8.0	22	0.1 - 1.5	1 - 48	0.1 - 10.0	274	Trakal *et al.* [2014]
Grape husks	600	2.0 - 8.0	22	0.1 - 1.5	1 - 48	0.1 - 10.0	178	Trakal *et al.* [2014]
Dairy manure	350	/	/	0 - 5.0	0 - 8	5.0	164	Xu *et al.* [2013]
Rice husk	350	/	/	0 - 5.0	0 - 8	5.0	29	Xu *et al.* [2013]
Plume stones	600	2.0 - 8.0	22	0.1 - 1.5	1 - 48	0.1 - 10.0	31.1	Trakal *et al.* [2014]
Nut shells	600	2.0 - 8.0	22	0.1 - 1.5	1 - 48	0.1 - 10.0	178	Trakal *et al.* [2014]
Digested animal waste	600	/	T_{room}	0.1 and 1.0	0 - 24	2.0	51.8	Inyang *et al.* [2012]
Sugarcane begasse	600	/	22	0.02 -1.0	0 - 24	2.0	6.22	Inyang *et al.* [2011]
Seawage sludge	550	2.0 - 5.0	25	0.5 - 5.0	4	4.0	31.1	Lu *et al.* [2012]
Bamboo	600	/	22	0.01 - 1.0	0.5 - 32	2.0	2.07	Zhou *et al.* [2013]
Bamboo + chitosan	600	/	22	0.01 - 1.0	0.5 - 32	2.0	12.4	Zhou *et al.* [2013]
Peanut hull + chitosan	600	/	22	0.01 - 1.0	0.5 - 32	2.0	0.62	Zhou *et al.* [2013]

TABLE 3.1: Overview of selected studies on Pb sorption by biochar (adapted from Trakal *et al.* [2014])

had suggested different mechanisms for the adsorption of Pb^{2+} by sludge-based biochar which includes:

1. The stabilization of Pb^{2+} was as a result of the precipitation on the surface coupled with physical adsorption.
2. Exchange of heavy metal with cations present in the biochar such as Ca^{2+}, Mg^{2+}, which relates to the inner complexation and precipitation with the mineral oxides and humic matter of biochar,it was demonstrated that this was the main sorption mechanism involved in their study.

Lu *et al.* [2012], further reiterated that the exchange of heavy metal with Ca^{2+}, Mg^{2+}, associated with sludge-based biochar was found to be the major mechanism responsible for sorption in their experiment;which led to the conceivable conclusion that under realalistic field conditions, the sorption mechanisms by biochar for soils contaminated by heavy-metals is most likely dependent on the soil-type and the cations present in it.

In studies conducted by Chan & Xu [2009],the authors did a review on *pH* values of biochar produced from different feedstock to obtain a *pH* of 8.1, with the use of similar

[0] / - (not indicated); T_{room} (*room temperature*).

feedstock material Wu *et al.* [2012] observed an increase *pH* values with pyrolysis temperature due to an increase in the biochar ash content.

Thus , it suffices to conclude that most biochars are alkaline material with a liming effect, which in-turn plays a role in reducing heavy metal mobility in contaminated soils [Sheng *et al.* , 2005].At equally high temperatures of pyrolysis, Cao & Harris [2010] found biochar produced from dairy manure to be effective in retaining *Pb* due to the its alkalinity and, thus its ability to faciltate insoluble *Pb* phosphate precipitation.

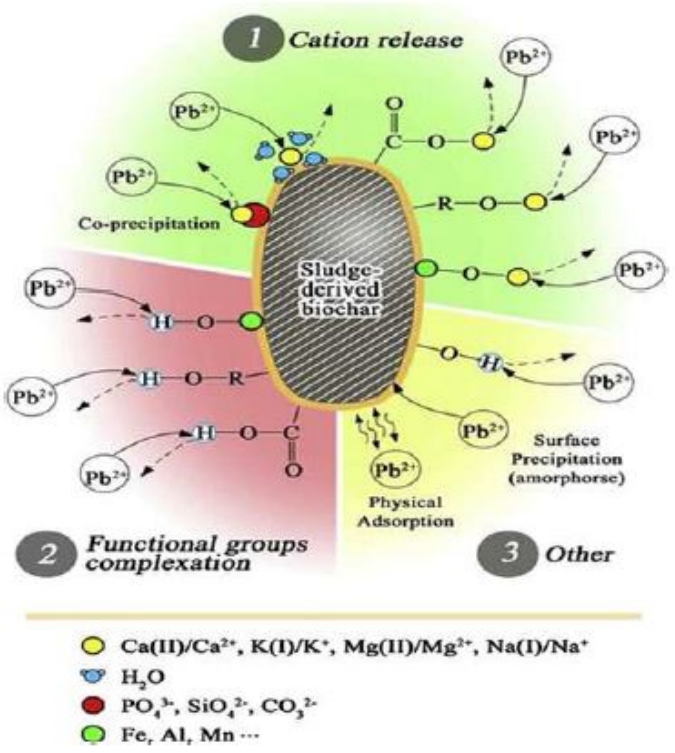

FIGURE 3.1: An illustration of possible mechanisms pathways of the adsorption of Pb on biochar.[Figure lifted from Lu *et al.* , 2012].

The *pH* of the soil is closely related to the bioavailability of heavy metals in soils. From the results of their study, Uchimiya *et al.* [2010] had suggested that biochar application to soil can go a long way in increasing soil *pH* and its cation exchange capacity, and thus subsequently enhance the immobilization of heavy metals in soil. In another experiment conducted by Ahmad *et al.* [2012], Mussel shell biochar was used to reduce *Pb* toxicity in a highly contaminated military shooting range soil in Korea. They recorded a 92.5% reduction in bioavailability of *Pb* in the soil with biochar treatment. They suggested the increases in the soil *pH* resulting from the liming effect of the biochar and the adsorption capacity were considered as the primary mechanisms of remediation effect of the biochar.

Chapter 4

Experimental Procedure

4.1 Materials

4.1.1 Preparation of The Adsorbate Solution

All chemical reagents used during this experiment were of high purity grades from Lach - Ner (Czech Republic).Stock solution of Pb(II) was prepared by dissolving (1000mgL^{-1}) of the desired quantity of $Pb(NO_3)_2$ (p.a) in a previously prepared background electrolyte of 0.01M $NaNO_3$ and 0.01M HNO_3 was used to adjust the pH of the solution.

4.1.2 Preparation and The Characterization of The Adsorbent

The adsorbent used in this study was made from waste agro-materials (Grape husk) belonging to the herbaceous and agricultural biomas (HAB) group.an agricultural biomass commonly found in central europe.Prior to its pyrolyis, physiochemical analysis was implemented to in order to determine the bulk density,moisture,material composition and ash content according to $TAPPI\ T264$ (1997) and $TAPPI\ T211$ (1993),followed by pH measurement using inoLab® pH-meter (7310 WTW,Germany),Carbon, hydrogen, oxygen,sulphur and nitrogen contents of the biochars were determined with the Flash EA 1112 aparatus in the CHNS/O configurtion (Thermo Fisher Scientific, USA).

To make the biochars (this part of the work carried out by previous studies by Trakal *et al.* [2014]), the homogenised and analysed grape husk waste agro-material were then slowly pyrolysed at 600°C in a muffled furnace under flow of Nitrogen. The resulting biochars were then cooled,ground, homogenised and sieved to 0.25–0.5mm sized particles. After rinsing several times with deionized water to remove impurities such as ash, the

grape-husk biochar (GHBC) were dried at 80°C during a 24h period for further analysis to determine its bulk-density, yield, moisture and ash content (see table 4.1).

Parameters		Value
pH	(-)	3.93 ± 0.06
A^d	(%)	6.43 ± 0.48
M	(%)	8.35
ρ	(%)	0.34 ± 0.01

Material composition		Value
T	(%)	17.06
R	(%)	19.01
L	(%)	23.65
C	(%)	34.01
Rest[$$$]	(%)	6.26

Elemental composition		Value
N	(%)	2.51
C	(%)	49.9
H	(%)	6.01
S	(%)	/[$]
O	(%)	35.1

TABLE 4.1: Physico-chemical characterization of the biomass before pyrolysis.

4.2 Batch Kinetic Sorption Experiment

4.2.1 Methods

In this experiment,batch kinetic studies were carried out to determine kinetics of the adsorption process.Optmum pH values and adsorbent dosage obtained from previous batch equilibrium sorption experiment by Trakal *et al.* [2014]

The Adsorption experiment involved filling a 1000ml glass beaker with 500ml of 209.8mg/l $Pb(II)$ ion solution and 0.01M $NaNO_3$ background electrolyte followed by the prepared biochar.The pH of solution was maintained at a desired value by adjusting it to a value of 5 with 0.01M HNO_3 acid solution and mixing on an orbital shaker at 25°C with a constant speed of 150 rpm.5ml of samples were withdrawn at predertermined contact times (2–840min).The experiments were performed in triplicate under equally defined

[0]bulk density (ρ_b), Moisture (M), tannin (T), Lignin (L), cellulose (C), the rest (Re), ash content (A^d).

and optimised conditions so as to ensure the reliability, accuracy and reproducibility of the collected data.The reaction mixture was then filtered through a 0.45μm membrane filter (VWR, Germany) and the concentration of Pb retained in the adsorbent phase analysed with the inductively coupled plasma optical emission spectroscopy (ICP-OES, Agilent).when preservation of the filtered samples was neccessary,it was neccessary to avoid the degradation of $Pb(II)$ concentration by reducing its pH below 2 with the use of $0.1M$ HNO_3 followed by preservation in the refrigerator at at low a temperature.

Chapter 5

Results and Discussion

5.1 Kinetic sorption rate

The Pb concentration sorbed by the adsorbent was calculated according to equation (5.1),where $V(l)$ is the volume of the solution, where $c_t(mgl^{-1})$ is the liquid-phase concentrations of $Pb(II)$ at time t and $m(g)$ is the mass of dry adsorbent used.

$$q_t = \frac{c_0 - c_t}{m} V \tag{5.1}$$

The sorption capacities of the $GSBC$ after different reaction times with initial concentrations of $Pb(II)$ ranging from $0.1mg.l^{-1}$ to $1mg.l^{-1}$ are shown in Figure 5.1. The maximum sorption capacities of the biochar improved with time as the initial $Pb(II)$ concentration increased. For the $0.1mg.l^{-1}$ initial $Pb(II)$ concentration, this maximum sorption could be interpreted as the equilibrium sorption, but as the initial $Pb(II)$ concentration the maximum sorpion could be interpreted as either saturation or point in the active sites of the biochar where the adsorped $Pb(II)$ undergoes a conversion process such as surface precipitation before attaining an equilibrium value, depending on the extent of the conversion process the trend uniformity in the final equilibrium sorption value for different initial $Pb(II)$ concentration would be affected, which explains the lowest equilibrium sorption capacity of $5.918mg.g^{-1}$ found after 24 hours for the highest studied initial $Pb(II)$ concentration of $1mg.g^{-1}$.
Despite the slow desorption process occuring at higher initial $Pb(II)$ concentration, the

[0]Initial $Pb(II)$ concentration (c_0), $Pb(II)$ concentration at any particular time T (c_t), an indication of the sorption capacity at any particular time t (q_t)..

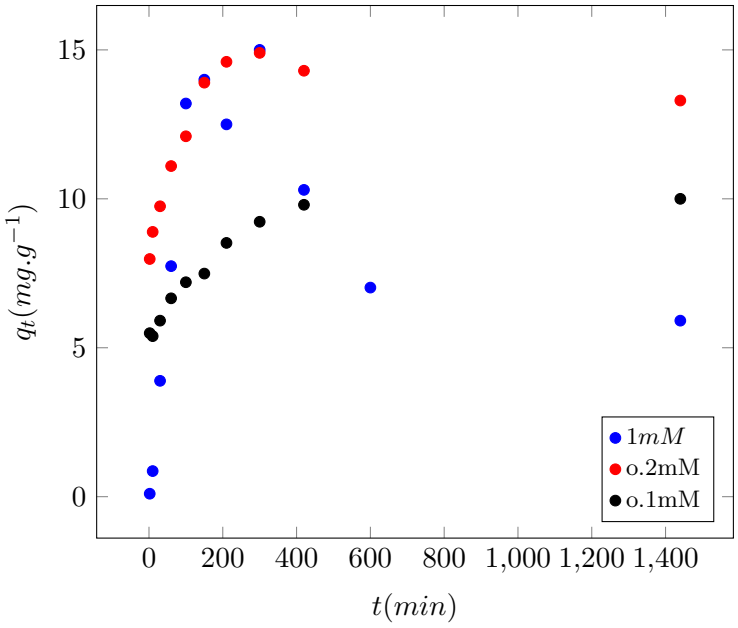

FIGURE 5.1: Sorption curves from experimental data of the sorption of different initial concentration of $Pb(II)$ ions onto biochar.

$1mM$ $10.77(mgL^{-1})$	2 (min)	10 (min)	30 (min)	60 (min)	100 (min)	150 (min)	210 (min)	300 (min)	420 (min)	600 (min)	1440 (min)
c_t (mgL^{-1})	10.76	10.70	10.46	10.15	9.71	9.65	9.77	9.52	9.94	10.21	10.30
q_t (mg/g)	0.1	0.86	3.89	7.74	13.2	14	12.5	15.6	10.3	7.02	5.91
$0.2mM$ $5.13(mgL^{-1})$	2 (min)	10 (min)	30 (min)	60 (min)	100 (min)	150 (min)	210 (min)	300 (min)	420 (min)	600 (min)	1440 (min)
c_t (mgL^{-1})	3.85	3.71	3.57	3.35	3.19	2.91	2.80	2.84	2.80	3.01	208
q_t (mg/g)	7.98	8.89	9.75	11.1	12.1	13.9	14.6	14.3	14.6	13.2	2.99
$0.1mM$ $4.97(mgL^{-1})$	2 (min)	10 (min)	30 (min)	60 (min)	100 (min)	150 (min)	210 (min)	300 (min)	420 (min)	600 (min)	1440 (min)
c_t (mgL^{-1})	2.67	3.24	3.07	2.83	2.66	2.57	3.24	2.01	1.83	1.62	1.77
q_t (mg/g)	5.49	5.39	5.91	6.66	7.20	7.49	8.52	9.23	9.80	10.4	10.0

TABLE 5.1: Changes in Concentrations (mgL^{-1}) and sorbed amount with time for different initial $Pb(II)$ concentration

time duration to attain equilibrium sorption was the same for all studied initial $Pb(II)$ concentration.

The initial rates of sorption were calculated using a plot of $q_t vs, t$ based on equation (5.2).According to the table 5.2 It is clear that the initial rate of sorption increases with the increase of initial $Pb(II)$ concentration, which is an expected scenario as a result of the increase in driving force at as concentration increases.

$$\frac{dq_t}{dt}|_{t=0} = -\frac{V}{m}\frac{dc_t}{dt}|_{t=0} \tag{5.2}$$

Initial concentration $Pb(II)$ (mM)	*Initial sorption rate* $(mg/g/min)$
1	0.10
0.2	0.038
0.1	0.015

TABLE 5.2: Effects of the initial $Pb(II)$ concentration has on the initial sorption rate

Initial concentration $Pb(II)$ (mM)	*Maximum sorption capacity* q_{max} $(mg/g/min)$
1	14.00
0.2	14.90
0.1	10.45

TABLE 5.3: Effects of the initial $Pb(II)$ concentration has on the *maximum sorption capacity* q_{max}

5.2 Parameter Estimation

The pseudo first- order kinetic models were fitted to the experimental kinetic data (q_t, the mass of adsorbed metal per g of dried sorbent (biochar) at different times).This was achieved by minimizing the squared sum of the deviations between the predicted and experimental values, by the use of the solver add-in with Microsoft's excel spreadsheet for windows. The pseudo second- order kinetic models were fitted to the experimental data by the use of a non-linear regression technique as described in table(5.5).

To check for accuracy of the model, a model goodness of fit was evaluated for the models by calculating the coefficient of determination (r^2),described in equation 5.3

with a data set of n values noted as q_i, each associated with a modeled value of f_n).

and $\bar{q}_i$, the mean of the measured data:

$$\begin{aligned} \bar{q} &= \frac{1}{n}\sum_{i=1}^{n} q_i \\ SS_{\text{tot}} &= \sum_i (q_i - \bar{q})^2, \\ SS_{\text{res}} &= \sum_i (q_i - f_i)^2 \\ r^2 &\equiv 1 - \frac{SS_{\text{res}}}{SS_{\text{tot}}}. \end{aligned} \tag{5.3}$$

5.3 Sorption Kinetic Models

The kinetic sorption models used in this thesis to describe the uptake of $Pb(II)$ by sorption on biochar are based on a kinetic pseudo-first and second order rate equation proposed by S.Lagergren [1898], and Ho [1995] respectively.

The difference between the First Order kinetic reaction and a Pseudo First Order kinetic reaction is the Pseudo first order kinetic reaction is a reaction that is supposed to occur by a higher order (higher than 1) but instead occurs as a first order due to the fact that the concentration of one of the reactant involved is much higher than the concentration of the other reactant.

Thus the concentration of the lower concentration reactant could be neglected and only the reactant of the higher concentration is used. Therefore, this makes the reaction tends to follow a first order kinetics instead of a higher order and it becomes the Pseudo First order reaction.

If the kinetic model best fits the sorption isotherm of the Pseudo first order by giving a r^2 value close to 1, then it indicates the reaction would be more inclined towards a physisorption process and similarly if the reaction were to fit well to the Pseudo second order kinetic model it shows an inclination towards chemisorption process.

Ho [1995] postulated a kinetic pseudo-second order rate law expression describing how the rate depends on the solid phase sorption capacity but not on the sorbate concentration.
In the present study, the experimental data for $Pb(II)$ sorption onto biochar were fitted to the simple, non- linear pseudo first-order kinetic model and non linear pseudo second-order expression. The expressions of the non-linear pseudo first and second-order kinetic model and and their linearized forms are shown in Table (5.5).

5.3.1 Simple First Order Model

A simple first order kinetic equation could be applied in describing the kinetics of sorption by considering the change in the bulk concentration of the sorption system with the use a simple first order rate equation given below:

$$c_t = c_0 \cdot e^{-K_1 t} \tag{5.4}$$

And in its linear form, equation (5.5) could be written as:

$$Log(c_t) = -\frac{K_1}{2.303} t + Log(c_0) \tag{5.5}$$

Where K_1 is the first order kinetic rate constant, (min^{-1}). The plots from the linearized version of the model $log\ c_t$ versus t (Figure 5.2) showed quite a wide disparity from a straight line.

This is an indication that the simple first order kinetic model isn't able to describe adequately this sorption process. However, similar results was obtained in the literature by Sparks [1989] and Hossain *et al.* [2005], They proposed that the simple first or second order models can not adequately be applied to adsorption system having solid surfaces which are rarely homogeneous surfaces, such as biochar, due to the fact that its almost impossible to experimentally separate the effect of chemical reactions and transport phenomena.

5.3.2 Pseudo First Order(Lagergren)Model

Its possible to model $Pb(II)$ sorption kinetics by the pseudo first-order equation, based on solid capacity, with the assumption that bivalent metal ion sorption onto the active site of the sorbent and its initial surface coverage is zero.
Thus, the sorption of $Pb(II)$ described by the first order kinetics could be represented as:

$$\frac{dq}{dt} = K_1(q_e - q) \tag{5.6}$$

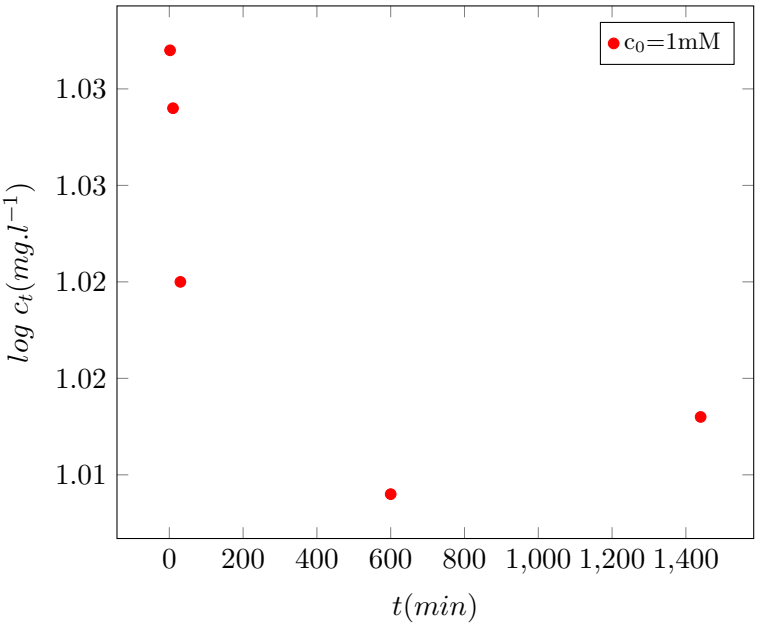

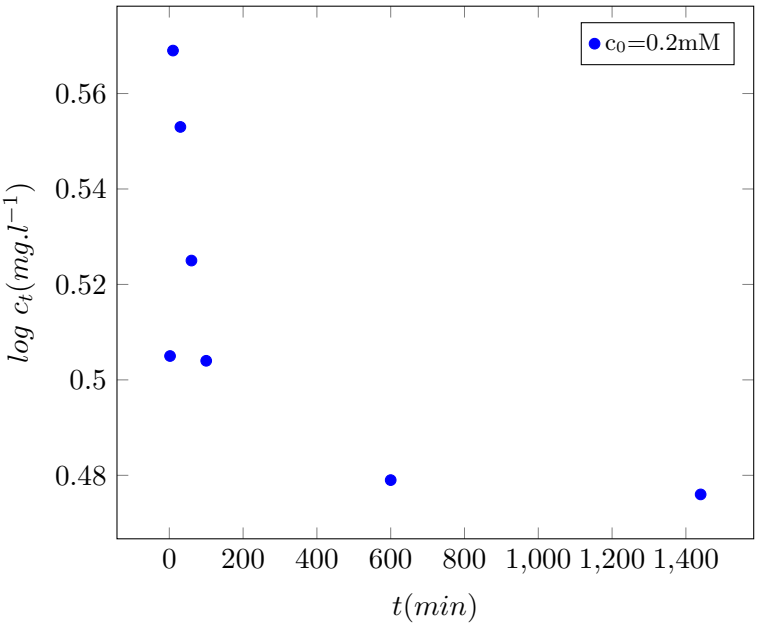

Integrating Equation (5.6) with boundary conditions $t = 0$; $q_t = 0$ and $t = t$; $q_t = qt$, gives:

$$q = q_e(1 - exp^{K_1 t}) \tag{5.7}$$

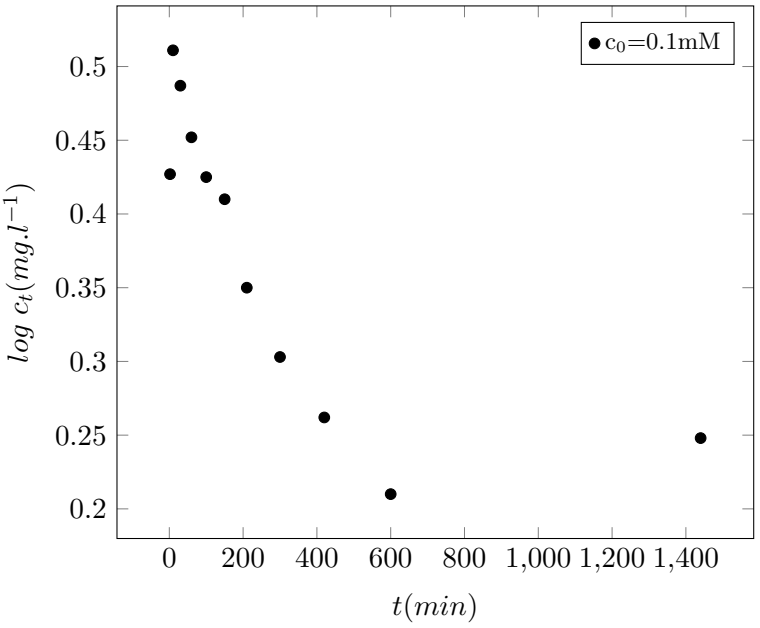

FIGURE 5.2: plot of $log\ c_t$ versus t for the deermination of the parameters of the simple first order kinetic model for $Pb(II)$ initial concentrations of $1mM$, $0.2mM$, $0.1mM$.

$$log(q_e - q) = log(q_e) - \frac{K_1 t}{2.303} \tag{5.8}$$

with q_e and q_t being the amounts of adsorbed metal ion (mg/g) respectively at equilibrium and at time t, and K_1 the pseudo first order rate constant (min^{-1}).

Intial concentration (mM)	K_1 min^{-1}	q_e $mg.g^{-1}$	r^2 (-)
1	0.032	-	0.99
0.2	0.014	-	0.99
0.1	0.0048	-	0.99

TABLE 5.4: The Pseudo first order kinetic parameters and correlation coefficient for $Pb(II)$ sorption at different concentrations.

The pseudo first order(Lagergren)model has been successfully used in experiments involving $Pb(II)$ sorption systems using sorbents such as composite biopolymer [Hideshi Seki, 1996], and kaolinitic clay [Orumwense, 1996].

Only the (pseudo first-order rate constant K_1) parameter and an impose value of q_e from experimental data was used to fit the pseudo first-order model, after series of optimisations, only the K_1 gave new values while the q_e remained the same.The data obtained was used to generate plots of q_t versus t(figure 5.3).

Thus, even though the data obtained from the kinetic model made quite a good correlation with experimental data, according to the high r^2 values given in table 5.4, this would not considered the dominant sorption mechanism.

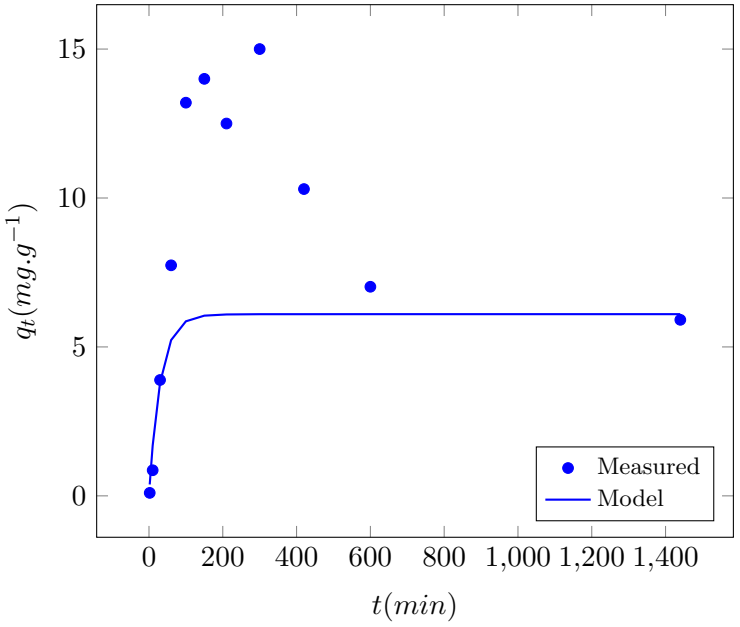

FIGURE 5.3: Sorption curves for the predicted pseudo first-order kinetics of the sorption of $1mM\ Pb(II)$ ions onto biochar.

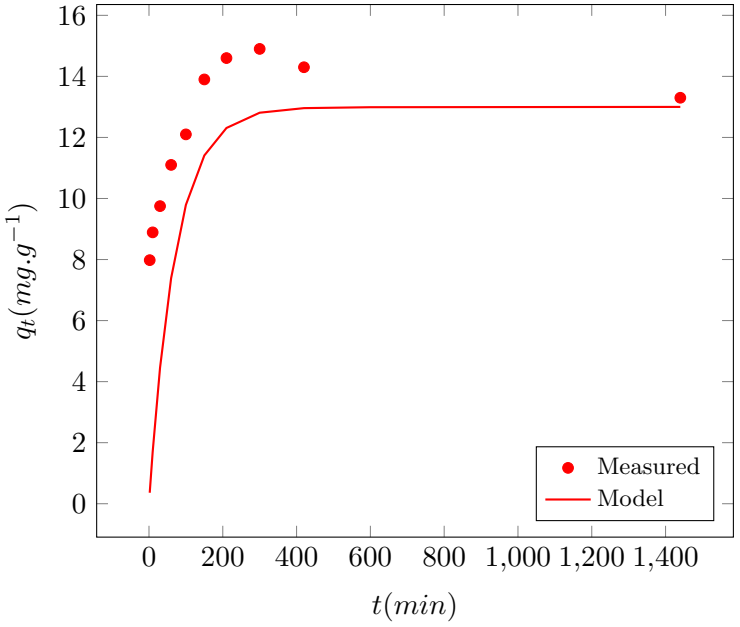

FIGURE 5.4: Sorption curves for the predicted pseudo first-order kinetics of the sorption of $0.2mM\ Pb(II)$ ions onto biochar.

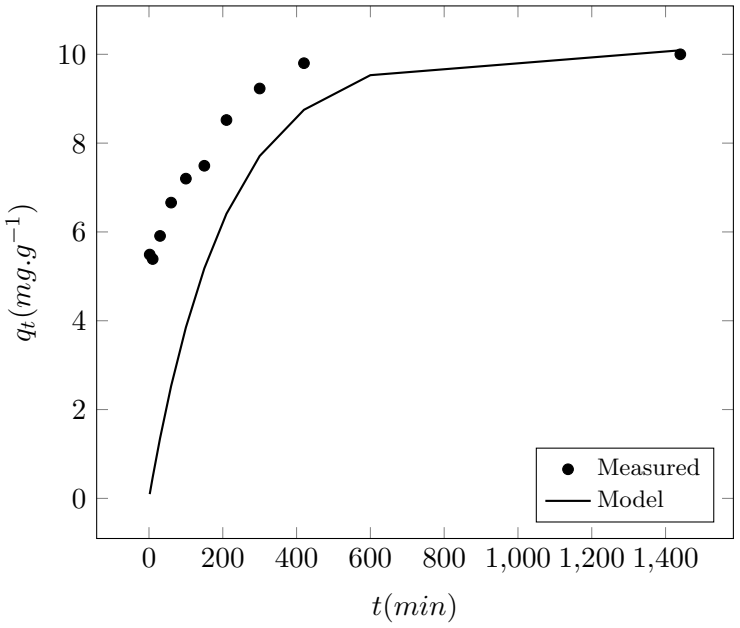

FIGURE 5.5: Sorption curves for the predicted pseudo first-order kinetics of the sorption of $0.1mM\ Pb(II)$ ions onto biochar.

Type	Non-linear form	linear form	Plot	Parameters
Pseudo first order	$q = q_e(1 - exp^{K_1 t})$	$log(q_e - q) = log(q_e) - \frac{K_1 t}{2.303}$	$log(q_e - q)$ *vs.* t	$K_1 = -2.303 \times slope$
Type1 Pseudo second order		$\frac{t}{q} = \frac{1}{K_2 q_e^2} + \frac{1}{q_e} t$	t/q *vs.* t	$q_e = 1/slope, K_2 = slope^2/intercept$
Type2 Pseudo second order	$q = \frac{K_2 q_e^2 t}{1 + K_2 q_e t}$	$\frac{1}{q} = \frac{1}{K_2 q_e^2} \frac{1}{t} + \frac{1}{q_e}$	$1/q$ *vs.* $1/t$	$1/intercept, K_2 = intercept^2/slope$
Type3 Pseudo second order		$\frac{1}{t} = \frac{K_2 q_e^2}{q} - \frac{K_2 q_e^2}{q_e}$	$1/t$ *vs.* $1/q$	$-slope/intercept, K_2 = intercept^2/slope$
Type4 Pseudo second order		$\frac{q}{t} = K_2 q_e^2 - \frac{K_2 q_e^2 q}{q_e}$	q/t *vs.* q	$q_e = -intercept/slope, K_2 = slope^2/intercept$
Type5 Pseudo second order		$\frac{1}{q_e - q} = \frac{1}{q_e} + K_2 t$	$1/(q_e - q)$ *vs.* t	$q_e = 1/intercept, K_2 = slope$

TABLE 5.5: Pseudo first and second-order kinetics and their linear forms (adapted from Ho [1995])

The data obtained showed good compliance with the pseudo- first order model which indicates physisorption due to weak bonding on the biochar by van der Waals forces and Multi-layer sorption are taking place.

5.3.3 Pseudo Second Order Model

if we assume the surface of the biochar particles to contain polar functional groups such as phenols, aldehydes, ketones and acids, which could be involved in the chemical bonding and also responsible for the $Pb(II)$ exchange capacity, then the reaction may be described in two ways, as was proposed by Coleman *et al.* [1956]:

$$M^{2+} + 2P^{-} \rightleftharpoons MP^{2} \tag{5.9}$$

or

$$M^{2+} + 2HP \rightleftharpoons MP_2 + 2H^{+} \tag{5.10}$$

In this case, the M^{2+} is the metal ion, P^{-} and HP are the polar sites on the biochar surface.
Similar experimental investigation conducted by Trakal *et al.* [2014] after series of FTIR analysis proposed the complexation of $Pb(II)$ with the $GSBC$ as one of the sorption mechanism responsible, thus confirming the presence of acid functional groups in the $GSBC$ which implies the theory by Coleman *et al.* [1956] could also be applied to our work.

The pseudo-second order sorption rate constant depends on the concentration of $Pb(II)$ on the biochar surface and the amount adsorbed at equilibrium. Thus sorption kinetics following pseudo second-order kinetics can then be expressed by:

$$\frac{dp_t}{dt} = K[P_0 - P_t]^2 \tag{5.11}$$

$$\frac{d(HP)_t}{dt} = K[(HP)_0 - (HP)_t]^2 \tag{5.12}$$

P_0 and $(HP)_0$ represents the number of equilibrium sites available on the sorbent surface, P_t and $(HP)_t$ are the number of active sites occupied on the surface of the sorbent at any time t. The sorption kinetics following pseudo second-order kinetics becomes:

$$\frac{dq_t}{dt} = K_2(q_e - q_t)^2 \tag{5.13}$$

where K_2 is the sorption rate constant $(g/mg\ min)$, q_e and q_t are respectively the amounts of $Pb(II)$ sorbed onto surface of biochar at equilibrium and at any time t (mg/g). With the application of Separation of variables, Equation (5.13), gives:

$$\frac{dq_t}{(q_e - q_t)^2} = K_2 dt \tag{5.14}$$

Applying the boundary conditions $t = 0$; $q_t = 0$ and $t = t$; $q_t = q_t$, the integration of Equation (5.14), gives:

$$\frac{1}{(q_e - q_t)} = \frac{1}{q_e} + K_2 t \tag{5.15}$$

Equation (5.15) is considered to be the integrated rate law for pseudo-second order reaction and can be manipulated further to produce linearized versions as shown in table (5.5).Where, according to Ho & McKay [1998], $(K_2 q_e^2 = h)$ represents the initial rate of sorption.

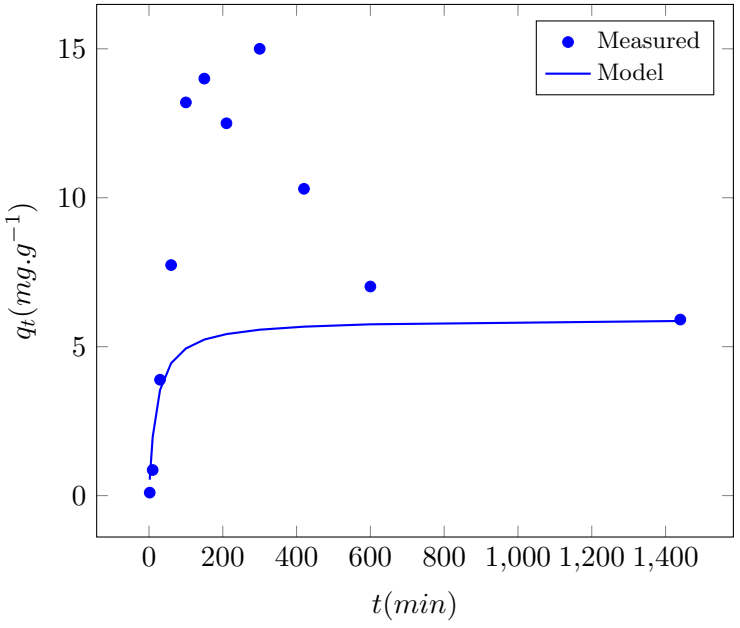

FIGURE 5.6: Sorption curves for the predicted pseudo second-order kinetics of the sorption of $Pb(II)$ ions to biochar.

The results obtained in table 5.6 showed the ability of the pseudo-second-order model to be able to predict the values of the K_2 and q_e with high values of r^2 which suggests

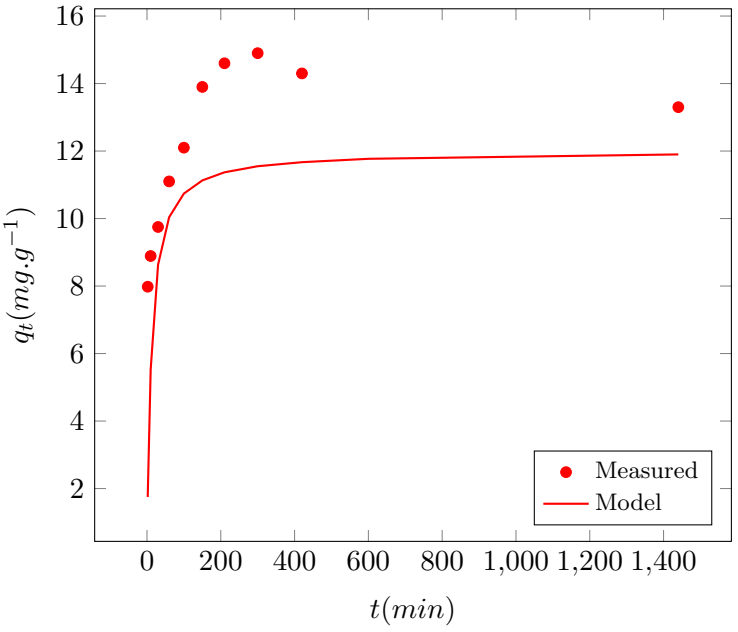

FIGURE 5.7: Sorption curves for the predicted pseudo second-order kinetics of the sorption of $Pb(II)$ ions to biochar.

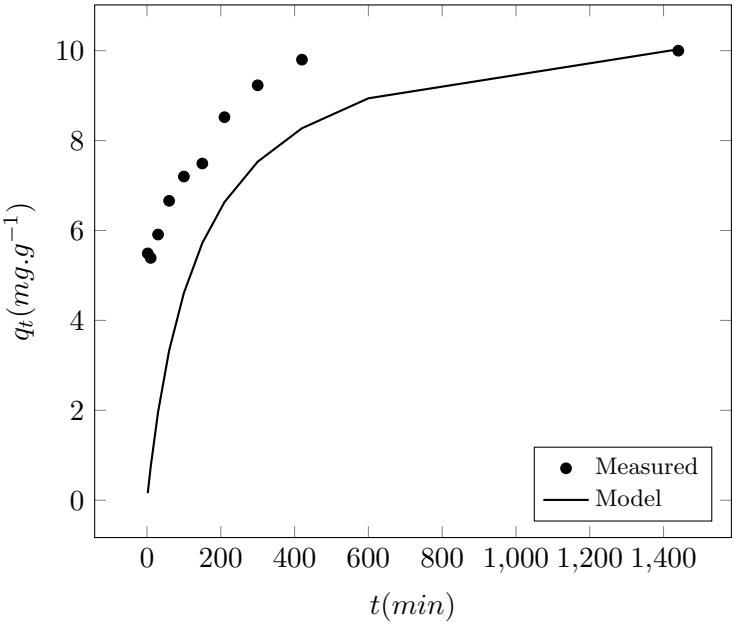

FIGURE 5.8: Sorption curves for the predicted pseudo second-order kinetics of the sorption of $Pb(II)$ ions to biochar.

Intial concentration (mM)	K_2 $g.mg^{-1}.min^{-1}$	q_e $mg.g^{-1}$	r^2 (-)
1	0.0083	5.95	0.99
0.2	0.0071	11.9	0.99
0.1	0.00066	11	0.95

TABLE 5.6: The Pseudo second order kinetic parameters, correlation coefficient and desorped amounts for $Pb(II)$ sorption at different concentrations.

that even though there was a pseudo-first-order reaction occuring simultaneously, the pseudo second-order kinetic model happened to be the more dominant mechanism. This confirms the presence of a chemical sorption occuring inline with the physical sorption, during chemisorption, the $Pb(II)$ get fixed to the surface of the biochar by forming a chemical covalent bond and finding sites that readily maximize their coordination number with the surface [O'Malley, 1983].

5.4 Quantitative Desorption Analysis

According to results obtained, it was found that at initial concentration of $0.1mM$, chemisorption and ion exchange processes was hypothesized to be the main sorption mechanism, but at relatively higher concentration, surface precipitation (either on the biochar pores or on the external surface) became important.
A possible scenario explaining sorption behavior at the higher initial $Pb(II)$ concentration is that the $Pb(II)$ is adsorped by the biochar and further creates a condition on the surface whereby additional $Pb(II)$ sorption could occur via surface precipitation(i.e., the first layer of Pb is by adsorption and additional layers are due to the formation of $Pb(II)$ precipitates loosely bonded to the biochar)[Yong, 2000].This is proven by Studies conducted by MacDonald [1994] which showed that the onset of $Pb(II)$ precipitation occurs as early as pH of 3.2.Correlating his findings with figure 5.9 (which shows that the initial concentration of the metal ion also contributes to the precipitation formation and thus desorption) and the result obtained in this thesis, indicates although a fixed pH value of 5 was used throughout the duration of the experiment, different initial concentration of $Pb(II)$ was used, with the onset of precipitation occuring from the $0.2mM$ and additional formation of precipitates occuring further as the concentration increased, thus the weak bonding of the $Pb(II)$ on the active sites of the biochar leading to its desorption.

It is clearly observed from the figure 5.6 that the desorption process are slower than the

sorption reactions.A possible reason for this could be due to the fact that the $Pb(II)$ undergoes a transformation from one state to another, i.e the conversion from an adsorbed species to a surface precipitate. moreover, it is well known that desorption reactions often require large activation energies, which cause the reaction to proceed slowly [McBride, 1994].

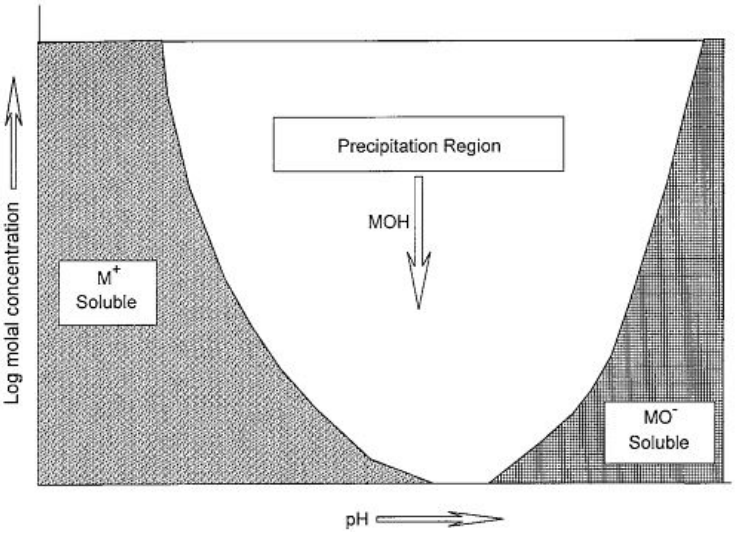

FIGURE 5.9: Solubility-precipitation for a metal hydroxide complex.[Figure lifted from Yong, 2000].

Inorder, to quantify the amount of $Pb(II)$ desorped from the biochar represented by the falling limb of the isotherm shown in figure 5.10 ,This portion of the sorption isotherm contributing to the desorption was fitted with a second order polynomial function given by equations(5.16) and (5.17) for the $1mM$ and $0.2mM$ $Pb(II)$ concentration respectively.

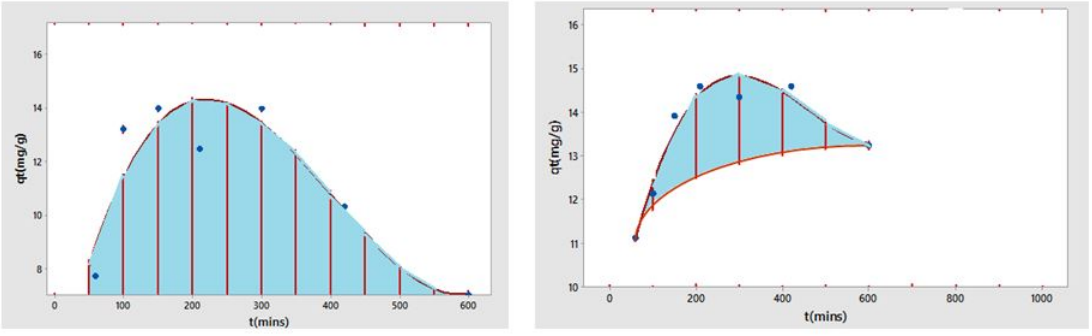

FIGURE 5.10: Rising and falling limb of the isotherm representing the sorption of $Pb(II)$ on biochar.

$$f(t) = 0.00009t^2 - 0.107t + 39.922 \tag{5.16}$$

$$f(t) = -0.00002t^2 + 0.0088t + 13.697 \tag{5.17}$$

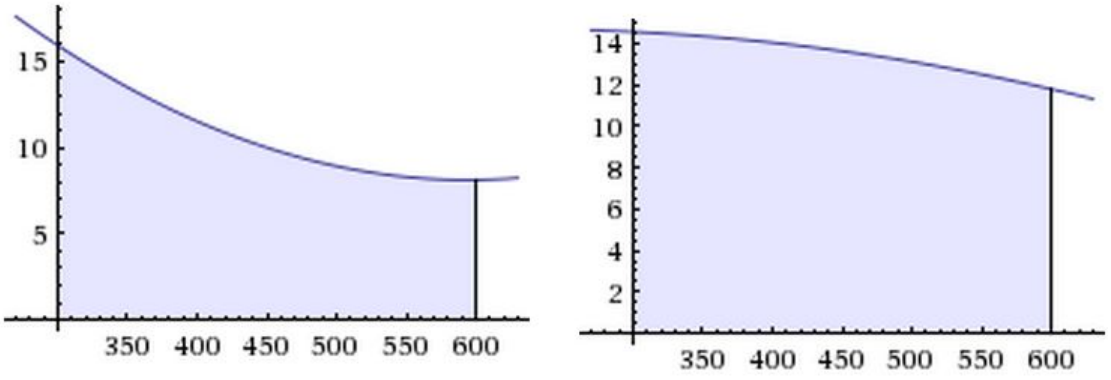

FIGURE 5.11: A Visual representation of the integral of the polynomial function of the desorped part of the isotherm.[Figure lifted from Lu *et al.* , 2012].

The method of the two-point Gaussian Quadrature is used to evaluate the function $f(t)$ and to approximate the total area (integral) of the falling limb of the isotherm.This was estimated by evaluating the function $f(t)$ within two points: $t = t_1$ and $t = t_2$ and multiplying it by constants c_1 and c_2. the formulas for the calculation are shown in equation (5.18), the area of the rectangular base is further subtracted from the total area obtained from the Gauss quadrature procedure and an avearge value of the desorped amount is obtained by dividing this value by the time frame during which the desorption occured.The average desorped amount calculated is shown in table 5.7.

$$\int_a^b f(t)\,\mathrm{d}t \approx c_1 f(t_1) + c_2 f(t_2) \tag{5.18}$$

$$t_1 = \left(\frac{b-a}{2}\right)\left(-\frac{1}{\sqrt{3}}\right) + \frac{b+a}{2} \qquad t_2 = \left(\frac{b-a}{2}\right)\left(\frac{1}{\sqrt{3}}\right) + \frac{b+a}{2}$$

$$c_1 = \frac{b-a}{2} \qquad c_2 = \frac{b-a}{2}$$

Intial concentration (mM)	*Average desorped ammount* $mg.g^{-1}$	*Average desorped ammount* $\%of\ sorped$
1	3.70	26.4
0.2	0.43	3.1
0.1	-	

TABLE 5.7: The averaged desorped amounts for $Pb(II)$ sorption at different concentrations.

5.5 Cation Exchange Capacity

The sorbent's cation exchange capacity, which is a measure of how many negatively-charged sites are available in the sorbent. in this case, its also a measure of the biochar's ability to hold strongly the $Pb(II)$ and release other embedded cations.

in order to ascertain the contribution from cationic exchange to be one of the main responsible sorption mechanisms, it becomes necessary to quantify the amounts of released cations (Na^+, Mg^{2+}, Ca^{2+} and K^+) from the biochar.Analysis of the cations released into the supernatant after Pb sorption (Table 5.8) gave an indication of the release of significant concentrations of K^+ which in practical situations would be the amount leached to the groundwater or made bio-available as fertilizer component to the plant roots , while the Na^+ were presumed to be negligible due to its presence as electrolyte in the solution, the concentrations of Mg^{2+}, Ca^{2+} were found to be insignificant.

The released mono-valent cations such as K^+ could only possibly be due to the electrostatic ion exchange with the $Pb(II)$, since they cannot form precipitates or possibly be combined with surface functional groups of the biochar.While, the divalent cations released such as Mg^{2+} and Ca^{2+} possibly originates from R-COO-Me which is the complexated surface functional groups, as well and the Mg^{2+} and Ca^{2+} precipitates on the biochar surface.

The acidic environment during the $Pb(II)$ sorption leads to the formation of precipitates and complexes which may be dissociated and thus leading to the formation of stable new $Pb(II)$ complexes or precipitates.

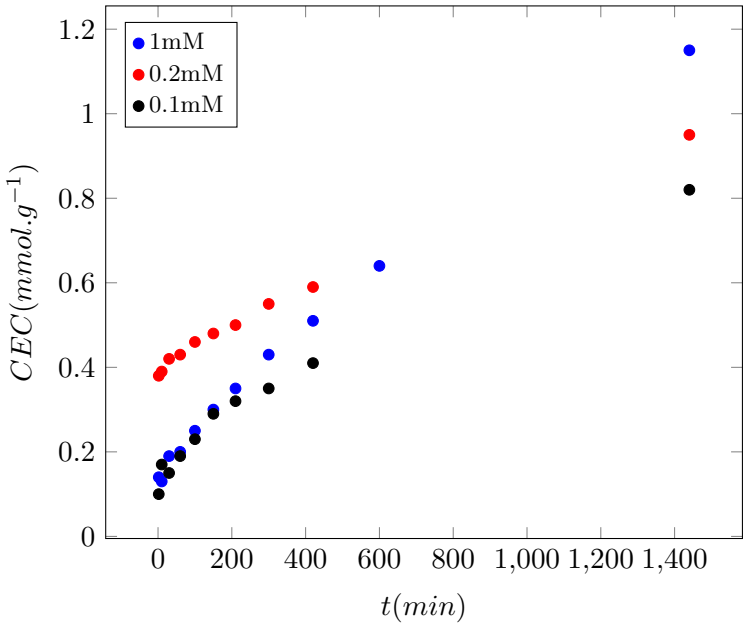

FIGURE 5.12: The evolution of the total cation release during $Pb(II)$ adsorption by GSBC at different initial $Pb(II)$ concentration

Figure (5.12), shows the evolution of the cation release(comprising summed releases of Mg^{2+}, Ca^{2+} and K^{+} cations), the CEC increased with the increase of $Pb(II)$ concentration, this was not the case with the 1mM $Pb(II)$ at the initial duration of the sorption.This anomaly could have resulted from the precipitation reactions due to the relatively high initial $Pb(II)$ concentrations used.The excess $Pb(II)$ concentrations occupied the biochar's active site within a very short time of the sorption experiment and this hindered the cation release thus the relatively lower cation exchange capacity until about 600 minutes when the equilibrium sorption had been attained and mechanical deoupling/deprecipitation from the biochar surface then the cation release equilibrated which explains the sudden increase and crossover in CEC as the $Pb(II)$ increased from $0.2mM$ TO $1mM$ as shown in figure (5.12).

Uniform increase of the CEC occurred when initial $Pb(II)$ concentration changed from $0.1mM$ to $0.2mM$. Therefore, the $Pb(II)$ that may have exchanged with the alkaline earth metals may as well formed very stable precipitates or complexes on the surface of the GSBC, as a result of the lower free energy which is required for metal complexation (Yin & Xu [2009]

The total amount of cations released into the solution during $Pb(II)$ sorption by the $GSBC$ was quite significant (Table 5.8).The result obtained confirmed that a cation exchange mechanism may have contributed an important role in $Pb(II)$ sorption onto biochar, with the oxygen containing functional groups such as carboxyl and hydroxyl being likely involved (Mohan *et al.* [2007]).

	2 (min)	10 (min)	30 (min)	60 (min)	100 (min)	150 (min)	210 (min)	300 (min)	420 (min)	600 (min)	1440 (min)
1*mM Pb(II)*											
Ca^{2+} (mM/g)	0.021	0.009	0.035	0.016	0.026	0.029	0.029	0.040	0.038	0.035	0.057
Mg^{2+} (mM/g)	0.003	0.002	0.002	0.002	0.002	0.002	0.002	0.002	0.002	0.002	0.003
K^{+} (mM/g)	0.119	0.114	0.149	0.184	0.221	0.267	0.316	0.390	0.468	0.602	1.090
cation release (mM/g)	**0.14**	**0.13**	**0.19**	**0.20**	**0.25**	**0.30**	**0.35**	**0.43**	**0.51**	**0.64**	**1.15**
0.2*mM Pb(II)*											
Ca^{2+} (mM/g)	0.004	0.006	0.017	0.010	0.015	0.012	0.014	0.019	0.023	0.029	0.045
Mg^{2+} (mM/g)	0.000	0.000	0.000	0.001	0.000	0.001	0.001	0.001	0.002	0.002	0.003
K^{+} (mM/g)	0.378	0.384	0.401	0.419	0.443	0.467	0.484	0.534	0.561	0.646	0.899
cation release (mM/g)	**0.38**	**0.39**	**0.42**	**0.43**	**0.46**	**0.48**	**0.50**	**0.55**	**0.59**	**0.68**	**0.95**
0.1*mM Pb(II)*											
Ca^{2+} (mM/g)	0.002	0.026	0.006	0.007	0.009	0.013	0.015	0.019	0.024	0.031	0.049
Mg^{2+} (mM/g)	0.000	0.006	0.001	0.001	0.001	0.002	0.003	0.003	0.004	0.004	0.005
K^{+} (mM/g)	0.095	0.143	0.143	0.179	0.219	0.279	0.299	0.333	0.385	0.456	0.766
cation release (mM/g)	**0.10**	**0.17**	**0.15**	**0.19**	**0.23**	**0.29**	**0.32**	**0.35**	**0.41**	**0.49**	**0.82**

TABLE 5.8: The cation release of Mg^{2+}, Ca^{2+} and K^{+} during $Pb(II)$ adsorption by GSBC at different initial $Pb(II)$ concentration.

5.6 Mechanisms of $Pb(II)$ Sorption

Due to the porous nature of biochar (Das *et al.* [2004]; Bonelli *et al.* [2007]), fitting the obtained experimental results to an intraparticle diffusion model could enable us to gain an insight into the mechanisms of sorption and the rate controlling steps affecting its kinetics.

Intra particle diffusion is used to describe a transport process which involves the movement of sorbate from the bulk of the solution to the sorbent.The intra-particle diffusion model used in this thesis is expressed as (Weber & Morris [1963]):

$$q_t = K_{id} \cdot (t)^{1/2} + C \tag{5.19}$$

where and K_{id} is the intraparticle diffusion rate constant $(mg/gmin^{1/2})$ obtained from the slope and C is the intercept, all obtained from the linearized plot of q_t vs. $t^{1/2}$ (Fig. 5.13).

The intercept of the plot which represents the intraparticle diffusion constant is related to the boundary layer effect.When the intercept is relatively large, the contribution of the surface sorption for the rate controlling step becomes large as well.

The determined values of the intraparticle diffusion coefficient K_{id} obtained is shown in Table 5.9

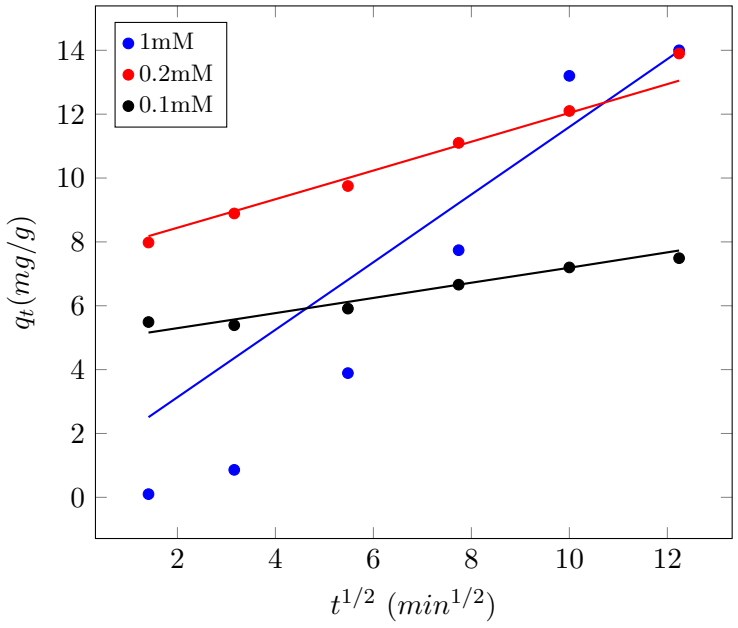

FIGURE 5.13: Linear plots for the pre-equilibrium data (lines) evaluating the intra-particle diffusion rate constant during $Pb(II)$ adsorption by GSBC.

c_0 (mM)	K_{id} $(mg/gmin^{1/2})$	C $(mg \cdot g^{-1})$	r^2 (-)
1	1.06	-1.02	0.899
0.2	0.45	7.54	0.952
0.1	0.24	4.82	0.961

TABLE 5.9: Calculated values of the intraparticle diffusion model during $Pb(II)$ adsorption by GSBC.

If the regression plots of q_t vs. $t^{1/2}$ is linear and also passes through the origin, then intraparticle diffusion could be established as the sole rate-limiting step.Even though the analyzed linear plots (Fig. 5.13) showed the lines corresponding to the initial concentrations of $0.2mM$ and $0.1mM$ $Pb(II)$ showed a strong linear dependency based on their relatively higher coefficient of determination (r^2), however the lines does not pass through the origin. This observation along with the fast sorption rate prior to reaching equilibrium for all iniial concentrations studied, suggests the intraparticle diffusion is not the rate controlling step.

Based on the overall results obtained, the $Pb(II)$ sorption mechanisms involved in this experiment could be attributed mainly to the following:

1 $Pb(II)$ exchange with K^+ and Na^+, attributed mainly to the electrostatic outer-sphere complexation;

2 Exchange of $Pb(II)$ with Mg^{2+} and Ca^{2+}, which could be attributed to co-precipitation and inner-sphere complexation with mineral oxides of GSBC;

3 Chemical sorption and surface complexation with free carboxyl and hydroxyl functional groups.

Chapter 6

Conclusions

The experimental and applied models results obtained from this study indicated that biochars which are produced from $GSBC$ (Grape stalks biochar) can be effectively used in removing heavy metals from porous media.

The kinetics of $Pb(II)$ sorption have been analysed by the use of a pseudo-first and second order kinetic model. Despite the partial fitting of the pseudo-first order kinetic model, The overall results obtained gave very good correlations judging from the high coefficient of determination.

maximum sorption capacities of of about $14mg.g^{-1}$ $15mg.g^{-1}$ and $10mg.g^{-1}$ $Pb(II)$ on $GSBC$ were attained for initial $Pb(II)$ concentrations of $1mM$ $0.2mM$ and $0.1mM$ respectively.

the results shows, and judging from the partial fitting of the first order kinetic model, Experimental and modeling results showed that $Pb(II)$ sorption onto $GSBC$ was controlled by multiple mechanisms including chemisorption, cation exchange and precipitation. The desorption which lead to the precipitation increased with the increase in intial $Pb(II)$ concentration.The desorption process removed 26% and 2.9% of maximum amount of sorped $Pb(II)$ for initial $Pb(II)$ concentrations of $1mM$ $0.2mM$ respectively, indicating the presence of reversible reactions. Thus, based on the data, obtained, If the Pb contamination in the porous media isn"t too high, $GSBC$ *biochar* may serve as a potential and appropriate alternative for the removal of toxic Pb from the porous media. Pb may precipitate in aqueous solution if its soluble concentrations tends to exceed about $0.2mM$ at a pH of 5, which leads to its desorption and resulting in potential groundwater contamination.Hence, it could be concluded that for the sorption system studied in this thesis, the bioavailability of $Pb(II)$ in the porous media such as soil or

groundwater environments would be relatively low if their concentration could be kept within the $0.1mM$ and $0.2mM$ levels and other conditions kept constant.

Appendix A

Sorption concentration Calculations for Pb(II) Sorption

Equation (5.1) is used to determine the sorped concentration at a particular time (q_t) in $mg.g^{-1}$ as follows:

$1mM$ *Initial concentration of* $Pb(II)$
Based on information from table (5.1)
Initial concentration c_0 of $Pb(II)$ in the solution = $10.77mgL^{-1}$.
V = volume of the sorped liquid phase = $0.5mL$ diluted with $9.5mL$ distilled water for total of $10mL$ analysed with the ICP-OES.
Initial concentration c_0 of $Pb(II)$ in the solution after dilution = $215.4mgL^{-1}$.
m =dry mass of the biochar sorbent = $0.8g$

$0.2mM$ *Initial concentration of* $Pb(II)$
Based on information from table (5.1)
Initial concentration c_0 of $Pb(II)$ in the solution = $5.13mgL^{-1}$.
V = volume of the sorped liquid phase = $1mL$ diluted with $9mL$ distilled water for total of $10mL$ analysed with the ICP-OES.
Initial concentration c_0 of $Pb(II)$ in the solution after dilution = $51.3mgL^{-1}$.
m =dry mass of the biochar sorbent = $0.8g$

$0.1mM$ *Initial concentration of* $Pb(II)$
Based on information from table (5.1)
Initial concentration c_0 of $Pb(II)$ in the solution = $4.97mgL^{-1}$.
c_t = concentration of $Pb(II)$ remaining in solution at any particular time (t)
V = volume of the sorped liquid phase = $1.5mL$ diluted with $8.5mL$ distilled water for total of $10mL$ analysed with the ICP-OES.
Initial concentration c_0 of $Pb(II)$ in the solution after dilution = $24.8mgL^{-1}$.
m =dry mass of the biochar sorbent = $0.8g$

Substituting the values above and values of c_t measured at at every predetermined time step in to equation (5.1), the corresponding sorped concentration (q_t) is obtained.

Appendix B

Determination of Parameters for Pseudo Second Order Kinetic Model

The parameters, K_2 and q_e were obtained using the non-linear pseudo second order equation by optimizing their values with the use of the coefficient of determination procedure outlined in equation (B.1).The values obtained were used to re calculate values to get the predicted values of q_t at different times.

$1mM$ $10.77(mgL^{-1})$	2 (min)	10 (min)	30 (min)	60 (min)	100 (min)	150 (min)	210 (min)	300 (min)	420 (min)	600 (min)	1440 (min)
q_t *model* $(mg.g^{-1})$	0.535	1.966	3.55	4.446	4.94	5.24	5.423	5.57	5.672	5.751	5.863
q_t *measured* $(mg.g^{-1})$	0.1	0.86	3.89	7.74	13.2	14	12.5	15.6	10.3	7.02	5.91
$0.2mM$ $5.13(mgL^{-1})$	2 (min)	10 (min)	30 (min)	60 (min)	100 (min)	150 (min)	210 (min)	300 (min)	420 (min)	600 (min)	1440 (min)
q_t *model* $(mg.g^{-1})$	1.75	5.53	8.63	10.04	10.74	11.13	11.37	11.55	11.67	11.77	11.9
q_t *measured* $(mg.g^{-1})$	7.98	8.89	9.75	11.1	12.1	13.9	14.6	14.3	14.6	13.2	2.99
$0.1mM$ $4.97(mgL^{-1})$	2 (min)	10 (min)	30 (min)	60 (min)	100 (min)	150 (min)	210 (min)	300 (min)	420 (min)	600 (min)	1440 (min)
q_t *model* $(mg.g^{-1})$	0.157	0.74	1.96	3.33	4.61	5.722	6.631	7.53	8.274	8.94	10.03
q_t *measured* $(mg.g^{-1})$	5.49	5.39	5.91	6.66	7.20	7.49	8.52	9.23	9.80	10.4	10.0

TABLE B.1: comparison of measured and second order kinetic model predicted values q_t at different time for different initial $Pb(II)$ concentration

$$\begin{aligned} \bar{q_t}measured &= \frac{1}{n}\sum_{i=1}^{n} q_t measured \\ SS_{\text{tot}} &= \sum_i (q_t measured - \bar{q_t} measured)^2, \\ SS_{\text{res}} &= \sum_i (q_t measured - q_t model)^2 \\ r^2 &\equiv 1 - \frac{SS_{\text{res}}}{SS_{\text{tot}}}. \end{aligned} \tag{B.1}$$

This procedure was also applied to the Pseudo first order model parameter optimization.

Appendix C

Experiment photographs

In this section, the experimental set-up as well as the equipment used is shown.

FIGURE C.1: $Pb(II)$ and biochar solution agitation – for sorption.

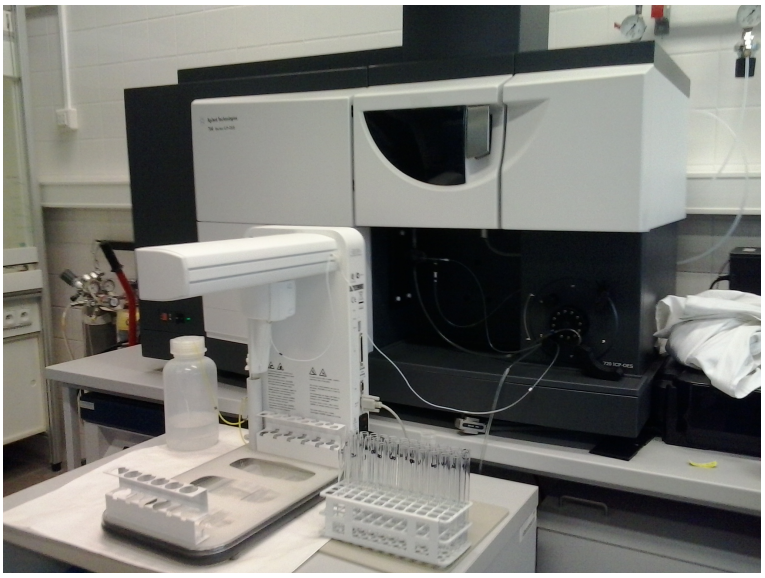

FIGURE C.2: Loaded standards and samples and ICP-OES instrumentation.

Bibliography

Ahmad, Mahtab, Soo Lee, Sang, Yang, Jae E., Ro, Hee-Myong, Han Lee, Young, & Sik Ok, Yong. 2012. Effects of soil dilution and amendments (mussel shell, cow bone, and biochar) on Pb availability and phytotoxicity in military shooting range soil. *Ecotoxicology and Environmental Safety*, **79**(May), 225–231.

Al-Anber, Mohammed. 2011. Thermodynamics Approach in the Adsorption of Heavy Metals. *In:* Moreno Pirajn, Juan Carlos (ed), *Thermodynamics - Interaction Studies - Solids, Liquids and Gases*. InTech.

Anderson, Mary P. 1992. *Applied Groundwater Modeling: Simulation of Flow and Advective Transport*. Academic Press.

Batu, Vedat. 2006. *Applied flow and solute transport modeling in aquifers : fundamental principles and analytical and numerical methods /*. Boca Raton, FL :: Taylor & Francis/CRC Press,.

Bonelli, P. R., Buonomo, E. L., & Cukierman, A. L. 2007. Pyrolysis of Sugarcane Bagasse and Co-pyrolysis with an Argentinean Subbituminous Coal. *Energy Sources, Part A: Recovery, Utilization, and Environmental Effects*, **29**(8), 731–740.

Cao, Xinde, & Harris, Willie. 2010. Properties of dairy-manure-derived biochar pertinent to its potential use in remediation. *Bioresource Technology*, **101**(14), 5222–5228.

Celia, Michael A., Bouloutas, Efthimios T., & Zarba, Rebecca L. 1990. A general mass-conservative numerical solution for the unsaturated flow equation. *Water Resources Research*, **26**(7), 1483–1496.

Chan, K. Y., & Xu, Z. H. 2009. Biochar - Nutrient Properties and Their Enhancement.

Coleman, N. T., Mcclung, A. C., & Moore, David P. 1956. Formation Constants for Cu(II)-Peat Complexes. *Science*, **123**(3191), 330–331.

Cunha, M. da Conceição, & Nunes, Luis Miguel. 2011. *Groundwater Characterization, Management and Monitoring*. WIT Press.

Das, Piyali, Ganesh, Anuradda, & Wangikar, Pramod. 2004. Influence of pretreatment for deashing of sugarcane bagasse on pyrolysis products. *Biomass and Bioenergy*, **27**(5), 445–457.

der Zee, S.E.A.T.M. van, & Leijnse, A. 2013. Solute Transport in Soil. *In:* Hernandez Soriano, Maria C. (ed), *Soil Processes and Current Trends in Quality Assessment.* InTech.

Domenico, Patrick A., & Schwartz, Franklin W. 1997. *Physical and Chemical Hydrogeology.* 2 edition edn. New York: Wiley.

Ern, Alexandre, & Guermond, Jean-Luc. 2004. *Theory and Practice of Finite Elements.* 2004 edition edn. New York: Springer.

Fetter, C. W. 2000. *Applied Hydrogeology.* 4 edition edn. Upper Saddle River, N.J: Prentice Hall.

Fetter, C. W. 2008. *Contaminant Hydrogeology.* 2 edition edn. Long Grove: Waveland Pr Inc.

Freeze, R. Allan, & Cherry, John A. 1979. *Groundwater.* Prentice-Hall.

Hideshi Seki, Akira Suzuki. 1996. Adsorption of Lead Ions on Composite Biopolymer Adsorbent. *Industrial and Engineering Chemistry Research*, **35**(4).

Ho, Y. S., & McKay, G. 1998. A Two-Stage Batch Sorption Optimized Design for Dye Removal to Minimize Contact Time. *Process Safety and Environmental Protection*, **76**(4), 313–318.

Ho, Yuh-Shan. 1995. *Absorption of heavy metals from waste streams by peat.* Ph.D thesis, University of Birmingham.

Hossain, Mohammad Abul, Kumita, Mikio, Michigami, Yoshimasa, & Mori, Shigeru. 2005. Optimization of Parameters for Cr(VI) Adsorption on Used Black Tea Leaves. *Adsorption*, **11**(5-6), 561–568.

Inyang, Mandu, Gao, Bin, Ding, Wenchuan, Pullammanappallil, Pratap, Zimmerman, Andrew R., & Cao, Xinde. 2011. Enhanced Lead Sorption by Biochar Derived from Anaerobically Digested Sugarcane Bagasse. *Separation Science and Technology*, **46**(12), 1950–1956.

Inyang, Mandu, Gao, Bin, Yao, Ying, Xue, Yingwen, Zimmerman, Andrew R., Pullammanappallil, Pratap, & Cao, Xinde. 2012. Removal of heavy metals from aqueous solution by biochars derived from anaerobically digested biomass. *Bioresource Technology*, **110**(Apr.), 50–56.

Jirí Simunek. 2006. Contaminant Transport in the Unsaturated Zone. *Pages 22–1–22–46 of: The Handbook of Groundwater Engineering, Second Edition*. CRC Press.

Leij, Feike J., Van Genuchten, Martinus Th, Skaggs, R. W., Schilfgaarde, J. van, & others. 1999. Principles of solute transport. *Agricultural drainage.*, 331–359.

Lu, Huanliang, Zhang, Weihua, Yang, Yuxi, Huang, Xiongfei, Wang, Shizhong, & Qiu, Rongliang. 2012. Relative distribution of Pb2+ sorption mechanisms by sludge-derived biochar. *Water Research*, **46**(3), 854–862.

MacDonald, Elaine. 1994. Aspects of competitive adsorption and precipitation of heavy metals by a clay soil.

Makuch, Dirk Schulze. 2004. Advection, Dispersion, Sorption, Degradation, Attenuation. *Encyclopedia of Life Support Systems (EOLSS), Developed under the Auspices of the UNESCO, Eolss Publishers, Paris, France*, **Vol. II**.

Manuel Alejandro Salaices Avila, Roman Breiter. 2009. Modelling the Competitive Sorption Process of Multiple Solutes During their Transport in Porous Media. *Environmental Modeling and Assessment*, **14**(5), 615–629.

Mays, Larry W. 2010. *Water Resources Engineering*. 2 edition edn. Hoboken, NJ: Wiley.

McBride, Murray B. 1994. *Environmental Chemistry of Soils*. New York: Oxford University Press.

Mohan, Dinesh, Pittman Jr., Charles U., Bricka, Mark, Smith, Fran, Yancey, Ben, Mohammad, Javeed, Steele, Philip H., Alexandre-Franco, Maria F., Gómez-Serrano, Vicente, & Gong, Henry. 2007. Sorption of arsenic, cadmium, and lead by chars produced from fast pyrolysis of wood and bark during bio-oil production. *Journal of Colloid and Interface Science*, **310**(1), 57–73.

Neuman, Shlomo P. 1984. Adaptive Eulerian–Lagrangian finite element method for advection–dispersion. *International Journal for Numerical Methods in Engineering*, **20**(2), 321–337.

O'Malley, Rebecca. 1983. Physical chemistry, second edition (Atkins, P.W.). *Journal of Chemical Education*, **60**(2), A63.

Orumwense, Faraday F. O. 1996. Removal of lead from water by adsorption on a kaolinitic clay. *Journal of Chemical Technology & Biotechnology*, **65**(4), 363–369.

Pinder, George F., & Celia, Michael A. 2006. *Subsurface Hydrology*. John Wiley & Sons.

Sheng, Guangyao, Yang, Yaning, Huang, Minsheng, & Yang, Kai. 2005. Influence of pH on pesticide sorption by soil containing wheat residue-derived char. *Environmental Pollution (Barking, Essex: 1987)*, **134**(3), 457–463.

S.Lagergren. 1898. ABOUT THE THEORY OF SO-CALLED ADSORPTION OF SOLUBLE SUBSTANCES. **24**(4), 1–39.

Sparks, Donald L. 1989. 9 - Kinetic Modeling of Inorganic and Organic Reactions in Soils. *Pages 173–189 of: Kinetics of Soil Chemical Processes*. San Diego: Academic Press.

Sparks, Donald L. 2013. *Environmental Soil Chemistry*. Elsevier.

Sublet, Renaud, Simonnot, Marie-Odile, Boireau, Alain, & Sardin, Michel. 2003. Selection of an adsorbent for lead removal from drinking water by a point-of-use treatment device. *Water Research*, **37**(20), 4904–4912.

Trakal, Lukáš, Bingöl, Deniz, Pohořelý, Michael, Hruška, Miroslav, & Komárek, Michael. 2014. Geochemical and spectroscopic investigations of Cd and Pb sorption mechanisms on contrasting biochars: engineering implications. *Bioresource Technology*, **171**(Nov.), 442–451.

Uchimiya, Minori, Lima, Isabel M., Klasson, K. Thomas, & Wartelle, Lynda H. 2010. Contaminant immobilization and nutrient release by biochar soil amendment: roles of natural organic matter. *Chemosphere*, **80**(8), 935–940.

UNFAO, United Nations Food and Agriculture Organisation. 1997. *Seawater Intrusion in Coastal Aquifers: Guidelines for Study, Monitoring and Control*. Rome: Food & Agriculture Org.

Wang, Herbert F., & Anderson, Mary P. 1995. *Introduction to Groundwater Modeling: Finite Difference and Finite Element Methods*. San Diego: Academic Press.

Wang, Jim J. 2010. The Chemistry of Soils, Second Edition. *Vadose Zone Journal*, **9**(1), 198.

Weber, Walter J., & Morris, J. Carrell. 1963. Kinetics of Adsorption on Carbon from Solution. *Journal of the Sanitary Engineering Division*, **89**(2), 31–60.

Wu, Weixiang, Yang, Min, Feng, Qibo, McGrouther, Kim, Wang, Hailong, Lu, Haohao, & Chen, Yingxu. 2012. Chemical characterization of rice straw-derived biochar for soil amendment. *Biomass and Bioenergy*, **47**(Dec.), 268–276.

Xu, Xiaoyun, Cao, Xinde, & Zhao, Ling. 2013. Comparison of rice husk- and dairy manure-derived biochars for simultaneously removing heavy metals from aqueous solutions: role of mineral components in biochars. *Chemosphere*, **92**(8), 955–961.

Yin, Chan K., & Xu, Zhihong. 2009. *Biochar: Nutrient Properties and Their Enhancement*. http://www.routledge.com/books/details/9781844076581/. Yes.

Yong, Raymond. 2000. *Geoenvironmental Engineering: Contaminated Soils, Pollutant Fate, and Mitigation*. CRC Press.

Zhou, Yanmei, Gao, Bin, Zimmerman, Andrew R., Fang, June, Sun, Yining, & Cao, Xinde. 2013. Sorption of heavy metals on chitosan-modified biochars and its biological effects. *Chemical Engineering Journal*, **231**(Sept.), 512–518.